PRESSURE NON-UNIFORMITY IN HETEROGENEOUS FOODS

DURING HIGH PRESSURE PROCESSING

BY

JOSÉ ANTONIO MALDONADO UGAZ

A dissertation submitted to the

Graduate School-New Brunswick

Rutgers, The State University of New Jersey

In partial fulfillment of the requirements

for the degree of

Doctor of Philosophy

Graduate Program in Food Science

Written under the direction of

Dr. Mukund V. Karwe

And approved by

_____

_____

_____

_____

New Brunswick, New Jersey

May 2015

ABSTRACT OF THE DISSERTATION

Pressure Non-Uniformity in Heterogeneous Foods during High Pressure Processing

by JOSÉ ANTONIO MALDONADO UGAZ

Dissertation Director:

Mukund V. Karwe, Ph.D.

High Pressure Processing (HPP) has gained acceptance as a technology that improves the safety of food products with minimal changes on its organoleptic properties. It is generally assumed that the internal pressure distribution in foods during HPP is uniform. This may not be true for solids with hard inclusions, like meats with bones or for particulate foods, which could compromise their safety and shelf-life. Numerical simulations of stress distribution in a solid with a hard inclusion showed existence of pressure and shear stress gradients. Our work aimed at determining if these gradients would affect microbial inactivation. Additionally we attempted to develop a pressure sensor and a method to monitor microbial inactivation in real-time.

Model systems consisting of a gel with a wood rod inclusion, embedded glass wool, or plaster particles were inoculated with *Listeria innocua* or *Saccharomyces cerevisiae* and subjected to HPP. A FRET system composed of DPH and Nile red was investigated as a possible pressure sensor. Propidium iodide was used to monitor the inactivation of *Enterobacter aerogenes*.

No differences were found in the inactivation of bacteria at different positions in the gel with wood inclusion. However, 2% glass wool decreased the inactivation of bacteria by 1 log cfu/g compared to pure gel. Higher inclusion volumes caused further drops in the inactivation levels. The yeast inactivation decreased by 1 log cfu/g with 2% plaster, but at 27% it reverted to the levels of the pure gel. It was determined that stress gradients formed very close to the inclusions, and that pressure and shear would affect each organism differently.

The FRET system was not an adequate pressure sensor. Membrane rupturing was detected during pressurization and holding but not during depressurization. A larger-than-expected drop in fluorescence was observed after cycles at higher pressure and longer times. This drop couldn't be explained by volume expansion alone, and the drop was not instantaneous. We suspect this drop in fluorescence came from reversible disassociation of ribosomes, occurring after cell wall and membranes rupture.

Our research has begun to elucidate the mechanisms of microbial inactivation by HPP, which could help in designing more effective processes.

Acknowledgments

This research project wouldn´t have been possible without the involvement of several people. First, I would like to deeply thank Dr. Mukund Karwe for his support, mentorship, and patience during the last seven years of my M.S. and Ph.D. studies. It was a pleasure working in his lab and learning under his guidance (especially when he demanded a little bit of extra effort), and I am sure that he'll be extremely successful in his new position as Dean of International Programs at SEBS, Rutgers. I would also like to thank Dr. Abilash Nair and Yuta Miyazawa for carrying out the numerical simulations that provided a theoretical foundation to our work, and Dr. Donald Schaffner and Dr. Alberto Cuitiño for always providing input from their expertise in Food Microbiology and Solid Mechanics, respectively, which were fundamental for designing our experiments and interpreting the results. And I would like to thank Dr. Donald Schaffner, Dr. Kit Yam, and Dr. Alberto Cuitiño for serving on my thesis committee.

I would also like to acknowledge Dr. Maria Corradini and Dr. Gil-Soo Han for their input in designing the fluorescence measurement experiments during high pressure processing. I would also like to thank Dave Petrenka, Bill Sumal, and Frank Caira, who were extremely knowledgeable and helpful in repairing and giving maintenance to our high pressure units.

Also, I would like to acknowledge the National Institute of Food and Agriculture (NIFA) of the U.S. Department of Agriculture (USDA) for funding this project under award Nº 2009-65503-05799.

Finally, I thank all my family and friends for their support during the last seven years. I want to thank my lab mates – past and present – Meenakshi, Deepti, Swetha, Shalaka, Gabriella, Vidya, Nidhi, Tanya, Siddhi, Yijing, Neha, Soundharya, Lin, Noopur, Tina, Isha, Gabriel, Anand, Li, Rajay, Karthik, Siddharth, Ender, and Kiran, for their encouragement, input, and for creating an amazing work environment (even when grabbing my stuff in the lab!). I want to specially thank my parents, Patricia and Pacho, and my sister, María Fe, for their constant support and encouragement. Without it, it would have been impossible to work successfully abroad. And I want to thanks Lisa, for her support and being there for me in the last stage of this project.

Table of Contents

List of Tables

List of Figures

1. Introduction

This section includes some of the basic concepts of high pressure processing and its application in food processing. Sections 1.1, 1.5, and 1.6 are directly related to the work done in this project and are important to understand how the hydrostatic pressure applied on the surface of the food items generates internal stress in food materials, and how microorganisms react to high pressure.

1.1. High Pressure Processing

High pressure processing (HPP) is a non-thermal processing technology that has been proven capable of extending the shelf life and increasing the safety of food products (Rendueles *et al.*, 2011). Besides irradiation, it is the most advanced alternative physical processing technology, as commercially viable high pressure processes have already become available within the last 20 years (Hendrickx and Knorr, 2002). Some of the commercial high pressure processed food products include sliced ham, oysters, clams, guacamole, fruit juices, fruit purees, ready-to-eat meals, dips and salsas.

HPP of food products is done mostly in batch processes. Figure 1.1 shows a typical high pressure processing set up. During HPP, the product is placed inside a processing vessel, which is filled with the pressure transmitting medium (usually water), pressurized either by pumping more pressure transmitting medium into the vessel or by using a piston to apply pressure. Once the target pressure is achieved, it is held for a

predefined period of time and then released very suddenly (Sun, 2005), as shown in Figure 1.2. Along with pressure, the temperature of the pressurizing medium and of the food items also increase during pressurization. Due to this temperature increase, a gradient with the vessel volume is established during the holding time, causing the temperature of the medium and of the food product to drop slightly as heat transfer to the vessel wall takes place. Therefore, after the pressure release, the temperature of the medium and food drops to values below the initial temperature, due to cooling associated with decompression.

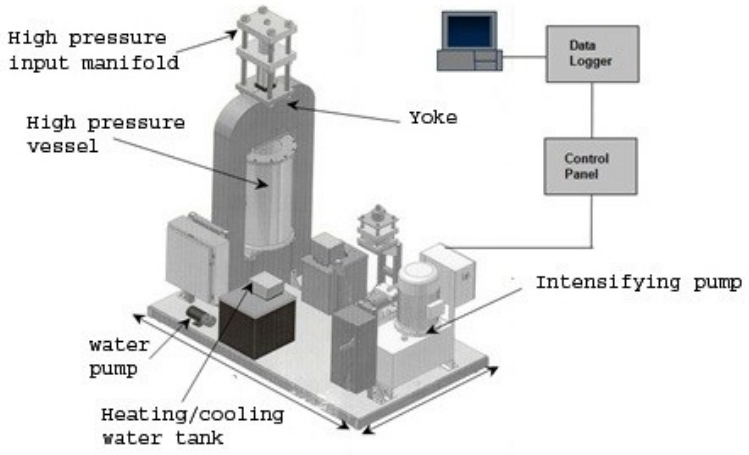

Figure 1.1: A typical high pressure vertical vessel with peripheral components (Courtesy: Elmhurst Research, Inc.)

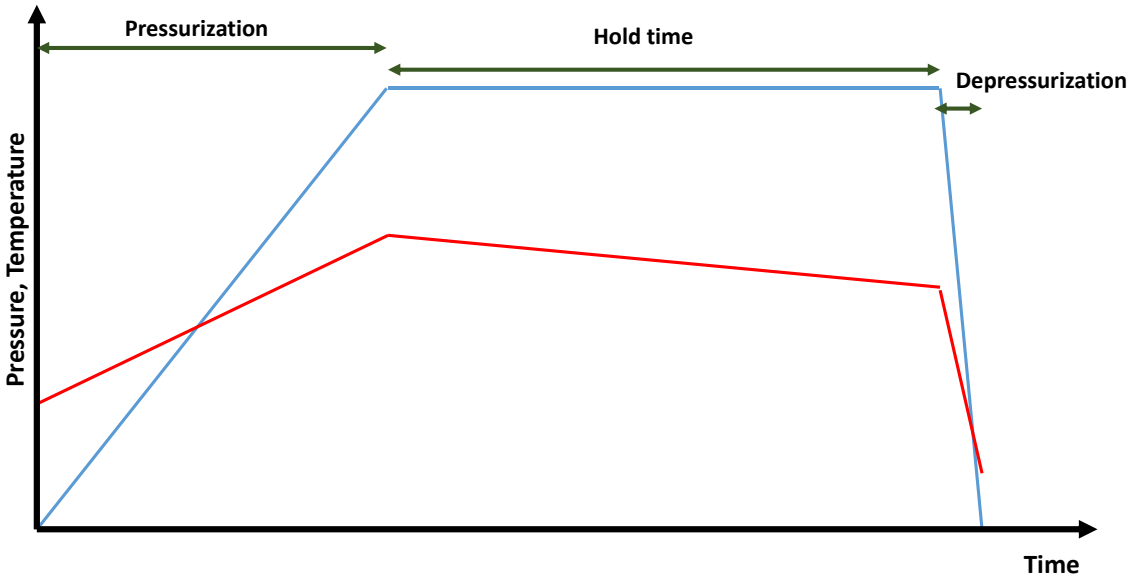

Figure 1.2: Diagram of pressure (blue line) and temperature (red line) during HPP.

One of the main advantages of HPP over thermal pasteurization, from the processing point of view, is that the pressure is considered to be transmitted uniformly and quasi-instantaneously throughout the sample, regardless of size, shape or packaging (Rendueles *et al.*, 2011; Doona and Feeherry, 2007; Brennan, 2006; Barbosa-Cánovas *et al.*, 2005; Sun, 2005). According to the reviewed literature, there are no limitations to the validity of these principles.

One of the main goals of HPP is to reduce the number of microorganisms in food products (Doona and Feeherry, 2007), in order to increase the safety and extend the shelf life of the products. HPP has been shown to cause relatively large reductions of vegetative cells in many different food products. For example, a 7 log cfu/mL reduction of *Staphylococcus aureus* was observed in apricot juice after HPP at 350 MPa for 5 min

at 30 ºC (Bayındırlı *et al.*, 2006), and a 7 log cfu/mL reduction of *Listeria Monocytogenes* was achieved in orange juice after HPP at 600 MPa for 5 minutes (Dogan and Erkmen, 2004). In other cases the achieved reduction has been much lower, such as 2.6 log cfu/g of *E. Coli* O103:H25 in dry-fermented sausage after 600 MPa for 10 minutes (Omer *et al.*, 2010), 2 log cfu/g of total aerobic mesophiles in clams after 545 MPa for 4 minutes (Narwankar *et al.*, 2011), 1.9 log cfu/g of a *Salmonella enterica* cocktail in peanut butter after 600 MPa for 18 minutes (D'Souza *et al.*, 2012), and 2.25 log cfu/g of *Salmonella Braenderup* in whole and cut tomatoes after 550 MPa for 2 minutes (Maitland *et al.*, 2011). All these results indicate that the microbial inactivation levels are highly dependent on the pressure and time of the process as well as the food matrix and the target microorganism. Small differences in the applied pressure can have large effects on the inactivation levels; for example, Koseki and Yamamoto (2007) measured a difference of 3 log CFU/g between the inactivation of *E. coli* ATCC 25922 at 300 MPa and 250 MPa at 15 ºC in peptone water suspension.

The temperature of the process also plays a role in the microbial inactivation (Buzrul *et al.*, 2008b; Teo *et al.*, 2001). Extensive research has been done on characterizing the heat transfer between the food items, pressurizing medium, and steel vessel and how it influences temperature non-uniformity during processing (Khurana, 2012; Zhang, 2011; Khurana and Karwe, 2009; Denys *et al.*, 2000a; Denys *et al.*, 2000b). This will be discussed in more detail in the next section.

Other applications for HPP of foods that have been researched include enhanced diffusivity of compounds into food matrices (Mahadevan and Karwe, 2011; Rastogi *et al.*, 2000; Rastogi and Niranjan, 1998) and the effect on bioactive compounds (Rawson *et al.*, 2011; Oey *et al.*, 2008a; Oey *et al.*, 2008b).

1.2. Heat transfer during high pressure processing

High pressure processing of foods is usually classified as a non-thermal technology; however it is necessary to be applied in combination with other treatments, usually heating, in order to achieve meaningful inactivation of bacterial and fungal spores. For example, Sale *et al.* (1970) carried out studies on spores of several species of *Bacillus* and achieved reductions no higher than 2 log cfu/mL of suspension after high pressure processing at 20 ºC for 1 hour and pressures between 100 and 800 MPa. On the other hand, Ananta *et al.* (2001) were able to achieve reductions of 6 log cfu/g of *Bacillus stearothermophilus* spores ATCC 7953 in mashed broccoli after high pressure process at 600 MPa and 120 ºC for 20 minutes.

The studies on the interaction between pressure and temperature in spores inactivation led to a petition to the FDA for the commercial use of pressure-assisted thermal sterilization (PATS) (Balasubramaniam, 2009). In the case of PATS, high pressure is only used as a means to reach the regular commercial sterilization temperatures, more rapidly and uniformly, through adiabatic compression heating. Farid (2006) filed a

patent application for a process in which thermal expansion due to heating in a closed container is used to generate pressure and apply heat to a food product, with the effects due to both pressure and temperature considered for microbial reduction.

Since the thermal effects are important in high pressure processing, especially when it is aimed at the inactivation of spores, it is of interest to know and control the temperature at which high pressure processing takes place and any temperature gradients that may arise during processing. Thermodynamics dictates that the temperature of most compressible substances will increase or decrease during compression or decompression, respectively. The temperature change when pressure is applied to a substance is given by:

$$\frac{dT}{dP} = \frac{T\alpha_P}{\rho Cp} \qquad (1)$$

where T is the temperature (K), P is the pressure (Pa), α_P is the thermal expansion coefficient (K^{-1}), ρ is the density (kg/m^3), and Cp is the isobaric heat capacity (J/kg·K). The inconvenience with using this equation is that density, heat capacity and thermal expansion coefficient are pressure and temperature dependent (Barbosa-Cánovas *et al.*, 2005). Figure 1.3 shows how density and heat capacity of water are pressure dependent, and is based on the NIST-ASME standard reference database 10 version 2.22 (Harvey *et al.*, 2010). Table 1-1 summarizes some of the findings of Buzrul *et al.* (2008a) and Rasanayagam *et al.* (2003), who determined the temperature increase (adiabatic compression heating) of several liquids during high pressure processing. In both cases

the initial temperature and pressure of the material, and the pressurization rate, were shown to influence the temperature increase rate.

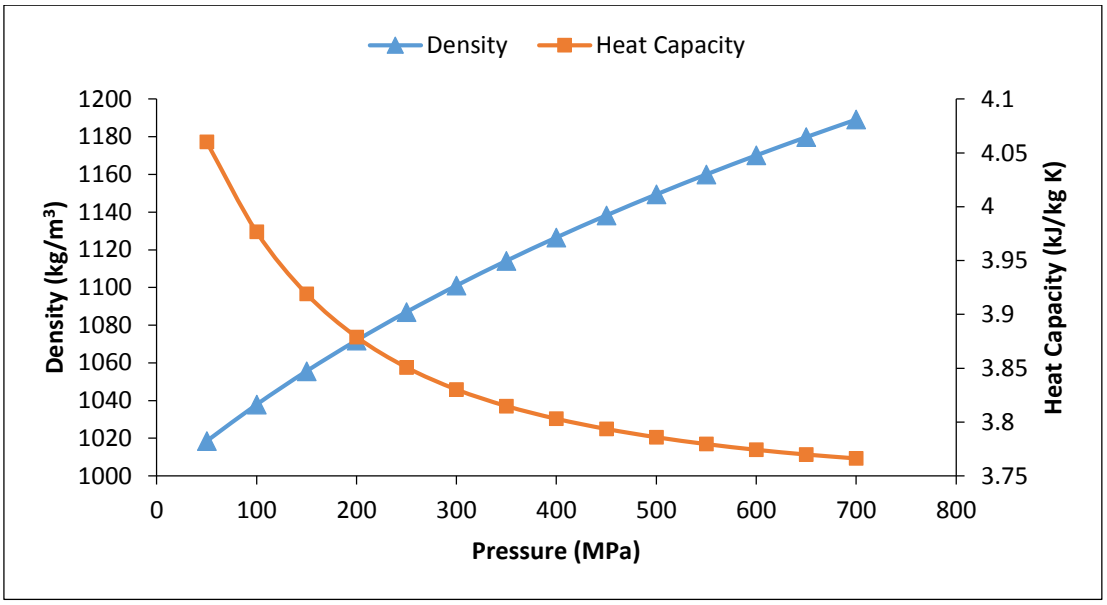

Figure 1.3: Density and heat capacity of pure water at 25 ºC between 50 MPa and 700 MPa (Harvey *et al.*, 2010)

Table 1-1: Temperature increase during HPP of selected substances

Substance	Temperature increase (ºC / 100 MPa)
Water[1]	2.8
Orange juice[1]	2.8
Skim milk[1]	3.1
Salmon fish[2]	3 ± 0.1
Whole milk[1]	3.3
Ethylene glycol[1]	3.7
Crude beef fat[2]	4.4 ± 0.8
Propylene glycol[2]	5.1 ± 0.5
Soybean oil[2]	6.3 ± 0.4
Olive oil[2]	7.2 ± 0.2
Ethanol[1]	8.2

[1] From Buzrul *et al.* (2008a).
[2] From Rasanayagam *et al.* (2003).

Pressure increases during the pressurization stage, and so does the temperature due to adiabatic compression heating. The pressure is then held constant for a specific amount of time in order to achieve the desired goal, followed fast decompression, as previously shown in Figure 1.2. Although the pressure inside the vessel remains constant during the pressure hold time, the average temperature normally decreases. As the temperature increases during pressurization due to adiabatic compression, a temperature gradient is established between the pressure transmitting medium and the colder vessel walls causing heat loss resulting in a temperature drop during the pressure hold step and a lower final temperature compared to the initial value.

Besides the heat transfer between the pressure transmitting medium and the vessel, there will also be temperature gradients between the different food components and between the food and the water; based on the adiabatic compression heating values of various components. Different components will reach different temperatures after pressurization, resulting in a complex and transient heat transfer process during the hold time. Zhang (2011) carried out numerical simulations to investigate the effects of food properties and packaging design in the temperature distribution during high pressure processing. Also, experimental evidence has been obtained that suggested that the temperature gradients established in a high pressure vessel would generate variability in reaction kinetics for enzyme and microbial inactivation (Hartmann and Delgado, 2003; Hartmann *et al.*, 2003; Hartmann and Delgado, 2002; Denys *et al.*, 2000b). This also indicates a potential use of certain enzymes as indicators of temperature uniformity in high pressure processing.

Several studies have been carried out aiming to model the temperature distribution during the pressure hold time. Hartmann (2002) carried out simulations on a 4 mL vessel, and determined that the pressurization rate strongly influences the temperature gradients developed inside the vessel, for example, a maximum difference of 8 ºC between two points inside the vessel at the end of the pressurization time was observed for a pressurization rate of 20 MPa/s while only a 6 ºC difference was observed for a pressurization rate of 10 MPa/s, for an initial temperature of 21 ºC and 500 MPa of pressure. They also determined that free convection would dominate the particle motions in the initial portion of the holding time, which was confirmed by Abdul

Ghani and Farid (2007) by simulating the temperature distribution in water and in a mixture of beef fat pieces and water at 25 ºC and 500 MPa of pressure. In this last study, it was also determined that the fat pieces would reach higher temperatures than the water, which is expected given that the adiabatic compression heating value of fat is higher than water. Pehl *et al.* (2002) studied the effect of viscosity on temperature gradients, and determined that a solution of 50% sucrose would develop gradients six times higher than those developed in water due to the higher viscosity. Khurana and Karwe (2009) conducted simulations of high pressure processing at different initial temperatures of the water, and determined that the temperature gradients would be higher at higher initial temperatures. Khurana (2012) studied the effect of different positions for the water inlet used to pressurize the vessel and different vessel orientations; it was determined that water inlet from the bottom would lead to more temperature uniformity in vertical vessels and that, in general, horizontal vessels would have a more uniform temperature distribution than vertical vessels.

A few studies have also been carried out aiming to reduce the temperature non-uniformity in the process. Knoerzer *et al.* (2007) studied the effect of a PTFE carrier inside the vessel for a process at 600 MPa and an initial temperature of 90 ºC, and determined that its insulating effect with respect to the vessel walls would increase the temperature uniformity, allowing for 94.6% of the carrier volume to achieve a 12 log cfu/g reduction of *Clostridium botulinum* spores; without the carrier no significant reduction was achieved. In subsequent studies, Knoerzer *et al.* (2010a) developed a software to optimize the wall thickness of a polymeric carrier in a high pressure unit,

aiming to maximize the heat retention and uniformity. Knoerzer *et al.* (2010b) developed and approach to screen for insulating materials with adiabatic compression heating values different than water, which would allow to better preserve the temperature inside the carrier as the carrier walls would also heat during pressurization. Khurana (2012) simulated the effects of a 12.7 mm PTFE insulation layer between the vessel wall and the pressurizing medium in a 10 L vertical vessel and in a 350 L horizontal vessel; the results for the vertical vessel are shown in Figure 1.4. A significant increase in temperature retention and uniformity was also observed in the horizontal vessel with an insulation layer.

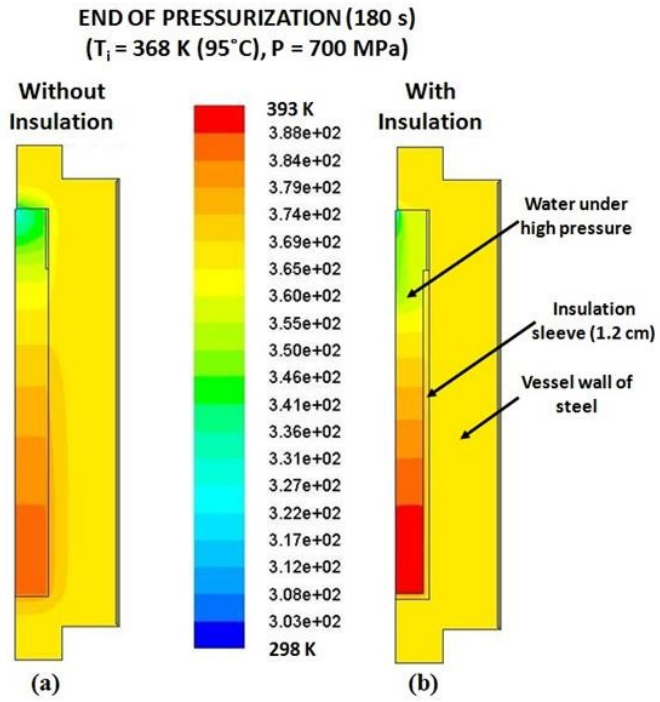

Figure 1.4: Isotherms in water and s.steel vertical vessel at Ti = 368 K, P = 700 MPa, Tinlet = 298 K, Q = 860,000 W/m^3 for (0 ≤ t ≤ 180 s), (a) without insulation, & (b) with insulation (12.7 mm thick) at the end of pressurization (180 s) (Khurana, 2012)

Pressure cycling has also been investigated as a method to increase the lethality of the process. In pressure cycling, instead of having a hold time at a constant high pressure, the pressure chamber would be depressurized and pressurized again, with very short periods of pressure hold and almost no lag in between the cycles. Pressure cycling has been found to be effective in enhancing microbial inactivation; Bradley *et al.* (2000), for example, found that pressure cycling increased the inactivation of lambda phage, a pathogen found in blood. Because the temperature after pressure release is lower than the initial temperature (see Figure 1.2), each cycle would start at a slightly

lower temperature than the previous one. Khurana (2012) investigated the temperature non uniformities during pressure cycling, and found that each cycle would have a slightly higher non uniformity compared to the previous one, as shown in Figure 1.5. The temperature non-uniformity was expressed in terms of coefficient of variation (COV).

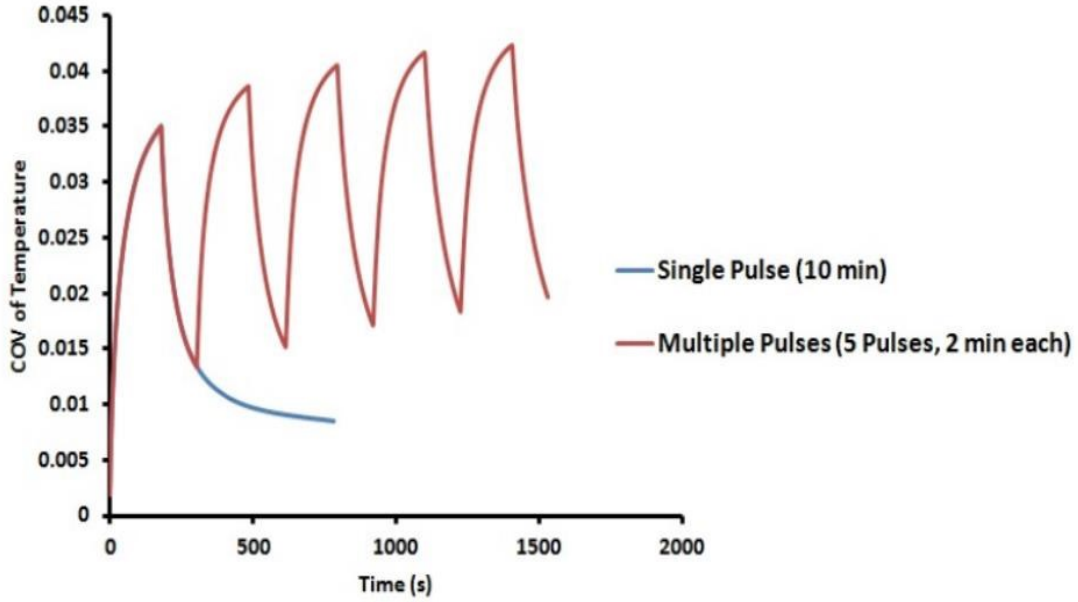

Figure 1.5: Coefficient of variance in a 10 L vertical vessel during high pressure processing at 700 MPa with initial temperature of 95 ºC (Khurana, 2012).

1.3. Mass transfer during high pressure processing

High pressure induced mass transfer has been explored as an enhancement over regular osmotic dehydration processes. Osmotic dehydration, which is a diffusion-based process, has been traditionally used in the food industry for partial removal of water

from fruits and vegetables and simultaneous infusion of small solute molecules such as sugar and salt, by immersing in concentrated solutions. Due to the difference between the internal and the external osmotic pressures, water diffuses out from the vegetable into solution while solute molecules from the concentrated solution diffuse into the food matrix. This is usually a slow mass transfer process that can take several hours or even days. High pressure processing has been shown to disrupt the cell membranes of the substrate, which may allow a much faster mass transfer process and therefore dramatically reducing the time needed.

One of the earliest works on cell permeabilization using high pressure processing was done by Dornenburg and Knorr (1993), who studied the recovery of pigments from plant cells. Rastogi and Niranjan (1998) observed that high pressure processing would increase the diffusivity of water and sugar by a factor of four and two, respectively, compared to untreated samples of pineapples. Rastogi *et al.* (2000) observed similar effects in potato cylinders, this time in the diffusivity of NaCl. They reported the use of the cell permeabilization index (Z_p) to characterize the effect of high pressure on the cell membranes, as follows:

$$Z_p = \frac{\left(\frac{\sigma_h^i}{\sigma_h^t}\right)\cdot\sigma_l^t - \sigma_l^i}{\sigma_h^i - \sigma_l^i} \qquad (2)$$

where σ is the electrical conductivity measured before processing (superscript *i*) or after processing (superscript *t*), at a low frequency (subscript *l*) or high frequency (subscript

h). The frequency values are dependent on the substrate. The value of Z_p varies between 0 for an intact cell system, and 1 for a completely disrupted cell system.

Additional work on enhancement of mass transfer with high pressure was done by Mahadevan and Karwe (2011), who observed that the infusion of quercetin into cranberries during high pressure processing was independent of the pressure applied between the range of 100 MPa to 500 MPa and that Z_p alone was not a good predictor of enhanced mass transfer coefficient, as high pressure would not increase the Z_p value for frozen-thawed cranberries and yet, higher amounts of quercetin were infused into these cranberries. Figure 1.6 and Figure 1.7 show the infusion of quercetin and Z_p values measured in this study. Figure 1.8 shows the loss of cellular structure after high pressure processing of frozen-thawed cranberries.

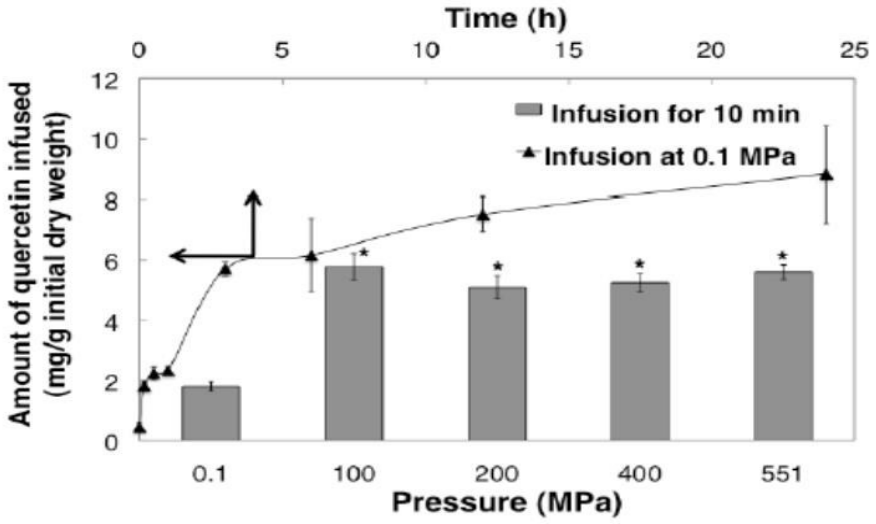

Figure 1.6: Quercetin infused in frozen-thawed cranberries at atmospheric conditions and during high pressure processing (Mahadevan and Karwe, 2011).

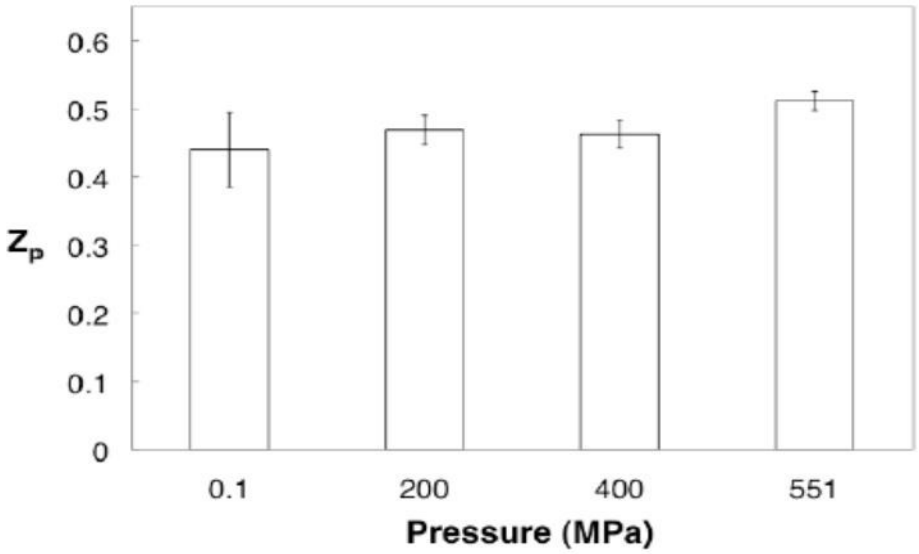

Figure 1.7: Zp values of frozen-thawed cranberries before and after high pressure processing (Mahadevan and Karwe, 2011).

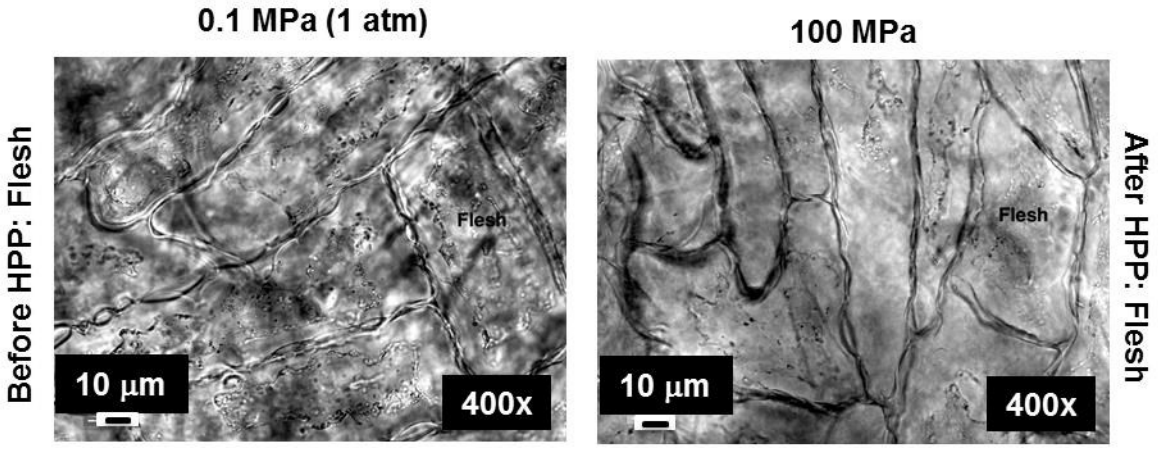

Figure 1.8: Microstructure of frozen-thawed cranberry flesh before (left) and after (right) high pressure processing (Mahadevan and Karwe, 2011).

The enhancement of mass transfer due to high pressure processing, at this point, has not attracted nearly as much attention as microbial inactivation, either by pressure alone or by the combination of pressure and heat. All the studies published so far point

out that the rate of mass transfer is greatly increased, and that this increase is dependent on the substrate and the solute. So far there is no general agreement on the mechanism by which high pressure enhances mass transfer.

1.4. Effect of high pressure on bioactive compounds

High pressure processing is a non-thermal technology that is promoted as to better preserve the fresh-like aspects of food products compared to regular thermal processing (Evolution Fresh, 2014); therefore it is of interest to determine if food bioactive compounds, especially those found in fruits, are retained after processing. This topic has attracted the attention of numerous researchers, and several studies and review papers (Rawson *et al.*, 2011; Oey *et al.*, 2008a; Oey *et al.*, 2008b) have been published on this topic.

In general, high pressure processing is considered to have little effect on covalent bonds (Rastogi *et al.*, 2007). Nonetheless, it influences the equilibrium of a reaction by favoring the direction in which the volume is reduced, either toward the products for reactions with negative reaction volumes, that is, when the volume of the products is lower than the volume of the reactants, or towards the reactants for reactions with positive reaction volume. Klärner *et al.* (1998) identified several cyclization reactions of 1-alkenes with negative reaction volumes; these could potentially affect the retention of bioactive compounds in fruits.

De Ancos *et al.* (2000) studied the carotenoid profile of persimmon fruits after high pressure and found significantly less degradation compared to thermal processing. In some specific pigments they observed an increase, and hypothesized that it could be due to disruption of cellular organelles or modification of the proteins that bound the carotenoids, which could enhance the release. Doblado *et al.* (2007) measured the vitamin C content and trolox-equivalent antioxidant capacity of high pressure processed germinated cowpeas, and observed an inverse correlation between them and pressure. Unlike these two studies, Fernández García *et al.* (2001) observed no decrease in antioxidant capacity, vitamin C or carotene content in orange, lemon and carrot juices, after high pressure processing.

Some insights on nutrient loss were obtained by Yen and Lin (1996). They measured vitamin C retention in thermally processed and high pressure processed guava purees, and observed a lower decrease right after processing for high pressured processed puree but faster degradation during storage. This suggests that high pressure retained vitamin C better than thermal processing, but at the same time the lower enzyme inactivation levels could have contributed to vitamin C loss during storage. Thakkar (2012) measured the ORAC antioxidant capacity, total phenolics and ellagic acid content of Muscadine grape juice after thermal pasteurization and a microbiologically equivalent high pressure processing, and found no difference between the treatments or with the unprocessed sample. After 8 weeks of storage at ambient temperature, the ellagic content in the high pressure processed sample had increased possibly due to hydrolysis of ellagitannins by enzymes not inactivated during processing.

The effects of thermal and high pressure processing on the antimutagenic activity of plant compounds have also been of interest. Butz *et al.* (1997) screened 14 fruits and vegetables using the Ames test and IQ carcinogen, and divided them in three groups: (i) resistant to both heat and pressure, like grapefruit and strawberry; (ii) resistant to pressure but not heat, like carrots, cauliflower, kohlrabi, leek, and spinach; and (iii) sensitive only to very high pressures, like beet and tomatoes. The effects of fermentation and high pressure extraction on the antimutagenic activity of deodeok and Korean barberry were studied (He *et al.*, 2010; Lee *et al.*, 2010). It was determined that high pressure extraction achieved the highest antimutagenic activities for fermented samples.

It is evident that more research is needed in this topic, especially if "healthier product" claims are desired for high pressure processed products so consumers would be willing to pay a premium price.

1.5. Effect of high pressure on microorganisms

As pointed out earlier in section 1.1, the processing parameters (pressure, holding time and sometimes temperature) required for the inactivation of different species of microorganisms are very diverse, which means that different bacteria will have different tolerance to pressure. In general, Gram negative bacteria are less resistant than Gram positive ones to pressure (Gould, 1995), likely because of the thicker and more rigid cell wall of the later compared to the former ones.

Modeling of microbial inactivation kinetics during high pressure processing often uses the parameters z_p and D_p adapted from kinetics of thermal inactivation, namely D and z values. Pavuluri and Kaur (2014) observed a log-linear kinetic for inactivation of *E. Coli* in black tiger shrimp between 300 MPa and 600 MPa for 3 min to 15 min and were able to calculate reliable values for D_p and z_p. Van Opstal *et al.* (2005) modeled *E. coli* inactivation in carrot juice also using those parameters; from their published data it can be determined that a decrease of 20 MPa at 20 ºC could increase the decimal reduction time by 25%. Zook *et al.* (1999) observed that the decimal reduction time of *S. cerevisiae* in orange juice at 20 ºC increased from 18 s to 50 s when the pressure decreased from 500 MPa to 450 MPa. However, in other cases, high pressure processing curves show tails, indicating that the inactivation by pressure it is not first order and rendering the concepts of D_p and z_p not useful (Earnshaw, 1995).

High pressure processing is often combined with other processing technologies in order to increase the inactivation or achieve levels of inactivation not possible by pressure alone (especially spores inactivation). A combination of high pressure and heat is perhaps the most studied combination technology; as mentioned before, heating is necessary if spores inactivation is needed; however, it is possible for pressure and temperature to be antagonistic. Ludwig *et al.* (1992) found that treatments for 10 min at 400 MPa and 5 ºC and 500 MPa at 25 ºC caused similar inactivation levels in *E. coli*. Antagonistic effects between pressure and heat have been observed in the inactivation of food enzymes. Van den Broeck *et al.* (2000) observed that above 900 MPa, pressure and temperature had an antagonistic effect on the inactivation of orange

pectinesterase. In the case of carrot pectin methylesterase, Ly-Nguyen *et al.* (2003) observed antagonistic effects below 300 MPa and above 50 ºC. Heremans (1995) observed, from the phase diagram of denaturation of proteins, that pressure stabilizes the protein against temperature denaturation at high temperature, and that at room temperature it was temperature that stabilized the protein against pressure denaturation, which would explain these last two results. Additionally, it could explain why pressure and temperature could be antagonistic in some cases in microbial inactivation, if it were due to protein denaturation. Hayman *et al.* (2008a) observed that the synthesis of heat shock proteins increased the pressure resistance of *Listeria monocytogenes*, which could also explain some of the antagonistic effects.

Other combination technologies that have been studied include high pressure and chemical preservatives, which have been used to inactivate *Salmonella* and *E. coli* in apple and orange juices (Whitney, 2005), and *Listeria monocytogenes* in sausages (Chung *et al.*, 2005). The combination of high pressure and sonication has also been studied, Abid *et al.* (2014) found that a sequential treatment of ultrasonication at 25 kHz and 70% amplitude and then HPP at 450 MPa for 10 min increased the inactivation of enzymes and caused full inactivation of aerobic mesophilic bacteria, yeasts and molds.

The growth stage of the organism and the temperature at which it grew have been found to have an effect in the inactivation levels from HPP. Isaacs and Chilton (1995) found that *E. coli* had approximately 5.5 log CFU/mL higher survival rate in stationary phase compared to mid-log phase after treatment at 200 MPa for 7 minutes.

Hayman *et al.* (2007) determined that *Listeria monocytogenes* grown at 15 ºC was significantly more pressure sensitive compared to cells grown at 4 ºC, 25 ºC, 35 ºC, and 43 ºC (which were the most resistant). They also determined that cells in mid-stationary phase were significantly more resistant than cells in exponential phase.

As mentioned before, numerous studies have been done on the inactivation of different bacterial species in foods, using different pressure, time, and temperature combinations. On the other hand, there are very few studies dealing with the mechanism by which high pressure inactivates microorganisms; one of the main reasons for this is the difficulty of carrying out *in situ* studies, that is, studying microbial cells in real time while they are being pressurized or depressurized, and not just before and after processing. The application of high pressure to cells triggers a series of events in the cells, not all of them necessarily lethal. Among the events studied, membrane damage has been observed in numerous studies and it has been suggested to be an important trigger of cell death during high pressure processing (Michiels *et al.*, 2008).

Perrier-Cornet *et al.* (1995) observed a permanent decrease by 10% of the volume of yeast cells after depressurization in an HPP cycle at 250 MPa for 15 min. Benito *et al.* (1999) studied the pressure resistance of different strains of *E. coli* 0157:H7 isolated from different outbreaks, and were able to determine that the more pressure sensitive strains also absorbed ethidium bromide and propidium iodide (fluorescent dyes) at a faster rate after high pressure processing compared to more pressure resistant strains, suggesting that the susceptible strains had sustained more membrane

damage. Additionally, the study indicated that the strains more resistant to pressure were also more resistant to acid, oxidative, and osmotic stresses. In another study, Perrier-Cornet *et al.* (1999) were able to differentiate the inactivated cells from the surviving cells after high pressure processing, and found a much larger volume reduction after decompression in the inactivated cells (35% volume loss) than in the surviving cells (10% volume loss). They also observed leakage of sodium, glycerol, calcium and potassium ions from the cells to the medium. Manas and Mackey (2004) observed a leakage of proteins and RNA in *E. coli* cells after the application of 200 MPa of pressure.

Hartmann and Delgado (2004) carried out numerical simulations of stress distribution of yeast cells during HPP, and concluded that Von Mises (shear) stress would develop at the cell wall and possibly disrupt it, but in the interior of the cell the stresses would be mostly hydrostatic; the effect on cell membrane was not included in this study. Although they did not experimentally verify their results, they found agreement with the experimental results obtained by Perrier-Cornet *et al.* (1999). In a relatively recent study, Black *et al.* (2007) determined that the minerals and ions associated with the casein micelles (calcium, magnesium, citrate, and phosphate) increased the pressure resistance of *Listeria innocua*, and hypothesized that the buffering capacity from phosphate and citrate ions, and membrane protection from calcium and magnesium would be the cause of this.

It has been observed that environmental conditions can affect the physical properties of the cell walls of bacteria, which could relate to their resistance to pressure

treatments. Thwaites and Mendelson (1985) and Thwaites and Surana (1991) studied the effect of different relative humidity levels on the cell wall of *Bacillus subtilis,* and observed that the Young's modulus and tensile strength of the cell wall decreased as the relative humidity increased; that is, at dryer conditions, the cell walls were less susceptible to be deformed or broken. Similar conclusions were reached by Nikiyan *et al.* (2010) for *Bacillus cereus* and *E. coli,* especially at RH levels below 84% for *E. coli* and below 65% for *Bacillus cereus*. This could explain the extreme resistance to pressure of several *Salmonella* strains in peanut butter, a very low moisture food, even though they were sensitive to pressure in peptone water suspensions (D'Souza *et al.*, 2012). In addition to cell wall strengthening, dehydration has also been shown to hinder the denaturation of proteins due to high pressure (Oliveira *et al.*, 1994), which could also explain the pressure resistance of Salmonella in peanut butter. Similar conclusion was reached by Hayman *et al.* (2008b), who observed an increase in the survival of *Listeria monocytogenes* and a decrease in the denaturation of lactate dehydrogenase at water activity values below 0.83 after high pressure processing.

Besides the physical rupture of the membrane, other changes that have been observed include permeabilization (that is, increased transfer of material from the cytoplasm to the medium) and inactivation of the F_0F_1 proton translocating ATPase (Michiels *et al.*, 2008). A review on the available literature regarding the effects of high pressure on biological molecules was published by Cheftel (1995); ATPase inactivation, conformation changes in macromolecules, ionic dissociation and pH changes in water,

changes in melting point and crystal structure were listed among the mechanisms studied that could be related to cell death.

Pressure has also been observed to cause dissociation of ribosomes (reversible at low pressures and irreversible at high pressures), inactivation of RNA polymerase and DNA gyrase (an enzyme involved in DNA replication), and condensation of the nucleotide (Michiels *et al.*, 2008). In a study with *Leuconostoc mesenteroides*, Kaletunç *et al.* (2004) determined that ribosomal denaturation was the main cause of cell death, but also observed the formation of blisters in the surface of cells, suggesting additional membrane damage. Isaacs and Chilton (1995) found areas devoid of ribosomes in *Listeria monocytogenes* after exposure to 250 MPa and enlarged fibrillar regions of DNA. Mentré and Hoa (2001) pointed out that high pressure has a stabilizing effect on DNA hydrogen bonds; this could hinder DNA transcription and therefore block the synthesis of vital proteins for the cell. Pope *et al.* (1975) measured the pressure sensitivity of protein synthesis in cells, and found them to be different between *E. coli*, *Pseudomonas fluorescens* and *Pseudomonas bathycetes.* They also concluded that the sensitivity changed with temperature. Wong and Heremans (1988) observed irreversible changes in the structure of chymotrypsinogen enzyme, due the reduction of α-helix and β-sheet substructures and the increase of random coil and turn conformations. They also observed that the pressure at which the denaturation started was higher when the pressurization rate was decreased. Additionally, Isaacs and Chilton (1995) found that the activity of isocitrate dehydrogenase, an enzyme from the respiratory cycle, had decreased by 75% after 2 minutes at 400 MPa in *E. coli*, which correlated with the

survival rate of the bacteria. Figure 1.9 and Figure 1.10 show the structures of a bacteria cell and yeast cell, respectively, to help understand the location of the elements discussed above. The cell sizes are 1 µm to 3 µm for bacteria and about 8 µm for yeast (Madigan *et al.*, 2006).

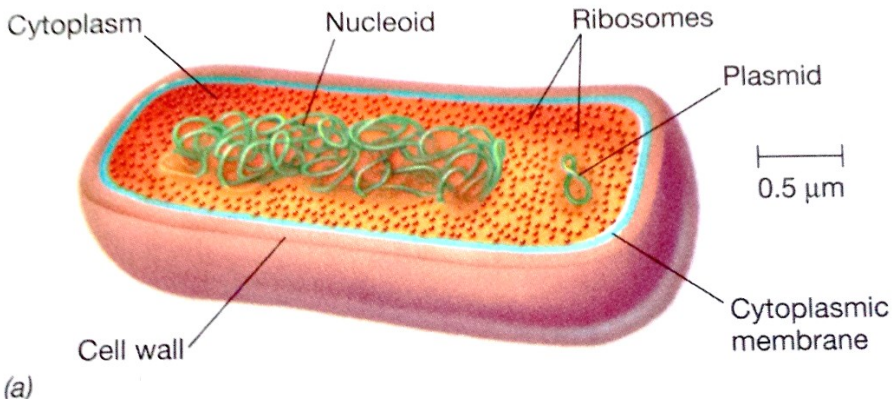

Figure 1.9: Diagram of a bacteria cell (Madigan *et al.*, 2006).

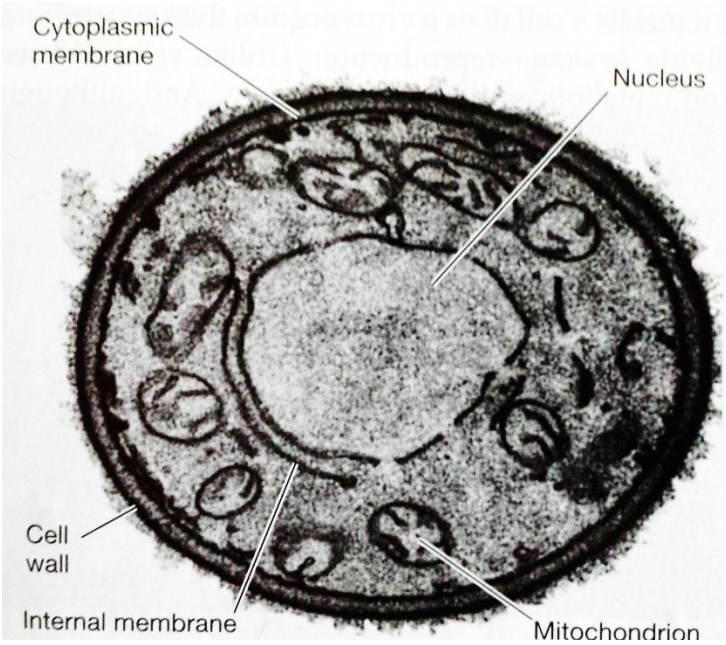

Figure 1.10: Electron microscope image of *Sacharomyces cerevisiae* (yeast) (Madigan *et al.*, 2006).

The published studies on high pressure effects on bacterial spores have not given a clear reason as to why they are so resistant to pressure (Reineke *et al.*, 2011). Nguyen Thi Minh *et al.* (2011) studied the effects of sporulation of *Bacillus subtilis* at different conditions, such as temperature, pH, and calcium content, and determined that they influenced the resistance of the spores to both high temperature and pressure. A similar study was done by Olivier *et al.* (2012) with other *Bacillus* species; however they found a negative correlation between developed temperature and pressure resistance at different sporulation temperatures, and found no trend between added minerals and resistance to pressure. Reineke *et al.* (2011), also working with *Bacillus subtilis,* were able to determine that the inactivation of spores during high pressure and temperature treatments first triggered the spore germination before inactivation took place.

It is clear that more research is needed on this topic, especially if high pressure processing is to be used to achieve commercial sterility in low-acid foods. Fortunately, the research on pressure tolerance of microorganisms to high pressure processing is also of interest to other disciplines, such as marine biology and astrobiology (and Sharma, 2011; Moeller *et al.*, 2008; Nicholson *et al.*, 2000), from which food science could benefit.

1.6. Hydrostatic pressure as a component of stress

When a solid object is in contact with other solids or fluids, it will be subjected to external forces or surface tractions, either concentrated at a point or distributed

throughout the surface (such as hydrostatic pressure), which will be transmitted from the surface to the interior of the solid. If an infinitesimally small area within the solid were isolated, the ratio of the force (F) to the surface area (ΔA) would be the stress vector (t):

$$t = \lim_{\Delta A \to 0} \left(\frac{F}{\Delta A} \right) \quad (3)$$

(Solecki and Conant, 2003).

If we were to isolate an infinitesimal volume element from that same body under external stress, we could find the stress vector for each of the faces of the element. Figure 1.11 shows such an element, with the vectors S_x, S_y, and S_z being the resultants of the stress vectors applied on both sides perpendicular to the x, y, z axes, respectively. Furthermore, we can decompose each of those vectors into three components (since we're using a Cartesian coordinate system); one of them perpendicular to the face and two of them parallel to the face. The stress components perpendicular to the face are known as normal stress (σ) and the components parallel to the face are known as shear stress (τ) (Popov *et al.*, 1976). The first subscript indicates the originating stress vector; the second subscript indicates the direction to which the component is parallel to.

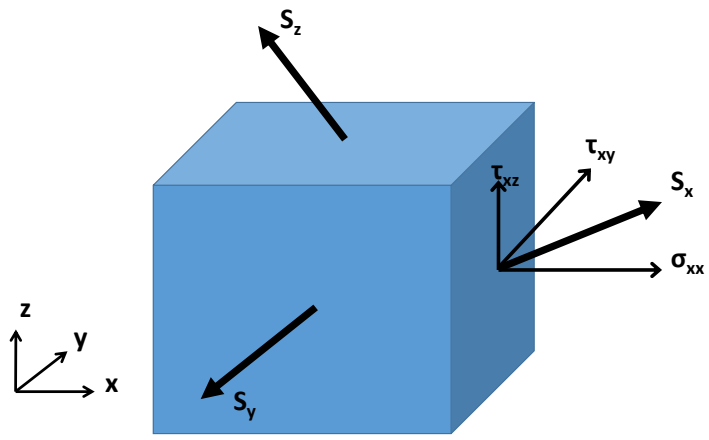

Figure 1.11: Stress Components in a Cartesian coordinate system

The decomposition of the stress vectors into their orthogonal components would be:

$$S_x = \sigma_{xx}\mathbf{i} + \tau_{xy}\mathbf{j} + \tau_{xz}\mathbf{k} \quad (4)$$

$$S_y = \sigma_{yy}\mathbf{j} + \tau_{yx}\mathbf{i} + \tau_{yz}\mathbf{k} \quad (5)$$

$$S_z = \sigma_{zz}\mathbf{k} + \tau_{zx}\mathbf{i} + \tau_{zy}\mathbf{j} \quad (6)$$

All these components can be arranged in a square matrix, called the stress matrix or stress tensor (σ), which is used in mathematical modeling and numerical methods. The main diagonal of the matrix contains the normal stresses, and the remaining elements are the shear stresses.

$$\sigma = \begin{bmatrix} \sigma_{xx} & \tau_{xy} & \tau_{xz} \\ \tau_{yx} & \sigma_{yy} & \tau_{yz} \\ \tau_{zx} & \tau_{zy} & \sigma_{zz} \end{bmatrix} \quad (7)$$

Since it is difficult to easily interpret the physical significance of the components of the stress-tensor, several invariant scalar measures of the stress-tensor have been

defined in-order to quickly characterize the nature of the force distribution within a solid. The most significant of these measures are the hydrostatic pressure component (P), which is intimately related to volume change of a specimen, and the effective stress deviator also known as the Von Mises stress (σ_{VM}), responsible for shape changes (Bower, 2010; Solecki and Conant, 2003). They are calculated as follows:

$$P = \frac{1}{3}\left(\sigma_{xx} + \sigma_{yy} + \sigma_{zz}\right) \quad (8)$$

$$\sigma_{VM} = \sqrt{\frac{\left(\sigma_{xx}-\sigma_{yy}\right)^2+\left(\sigma_{yy}-\sigma_{zz}\right)^2+\left(\sigma_{zz}-\sigma_{xx}\right)^2+6\left(\tau_{xy}{}^2+\tau_{yz}{}^2+\tau_{zx}{}^2\right)}{2}} \quad (9)$$

Both of these quantities are invariants of the stress tensor, which means they remain constant even if the coordinate system changes. This makes them very useful for finite element analysis, when the coordinate system of one element may not necessarily coincide with the coordinate system used for another element.

The relationship between stress and deformation or strain is represented using several elastic moduli. Figure 1.12 shows a solid in which stress is applied in a single direction; this causes it to compress along the y direction and to expand in the z and x directions.

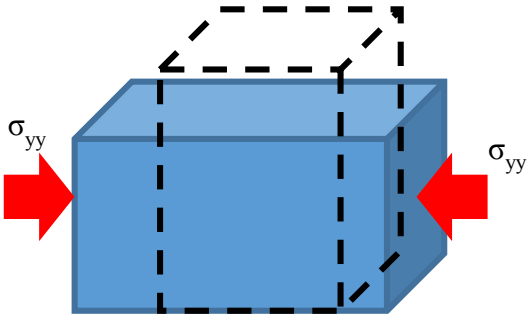

Figure 1.12: Solid under uniaxial stress

In this case the relationship between the stress applied in the y direction and the strain in that same direction (ε_{yy}, the change of length divided by the original length) would be represented as:

$$\sigma_{yy} = E \cdot \varepsilon_{yy} \quad (10)$$

$$\varepsilon_{yy} = \frac{1}{E}\sigma_{yy} \quad (11)$$

Where E is the Young's modulus or modulus of elasticity. This equation is true for linearly elastic materials, in which the value of Young's modulus remains constant for the range of stress being studied and the material bounces back to its original conformation after the stress is removed (Boudjema *et al.*, 2003). Although usually an example of a body under tension stress (which intuitively would cause the body to extend in that direction) is used to define the Young's modulus, nothing in the literature prevents that definition from applying to a body under compression stress (which would cause the body to compress in that one direction). We do expect that the ranges for linearity of equation (8) under tension and compression stress to be different.

The expansion in the other directions is known as the Poisson's effect. It has been experimentally observed that it is related to the compression in the direction in which the stress is applied.

$$\varepsilon_{xx} = -\nu \cdot \varepsilon_{yy} \quad (12)$$

$$\varepsilon_{zz} = -\nu \cdot \varepsilon_{yy} \quad (13)$$

In a system under normal stress in the 3 directions, the resultant deformations in the x, y, and z direction would be written as:

$$\varepsilon_{xx} = \frac{1}{E}\Big(\sigma_{xx} - \nu\big(\sigma_{yy} + \sigma_{zz}\big)\Big) \quad (14)$$

$$\varepsilon_{yy} = \frac{1}{E}\Big(\sigma_{yy} - \nu(\sigma_{xx} + \sigma_{zz})\Big) \quad (15)$$

$$\varepsilon_{zz} = \frac{1}{E}\Big(\sigma_{zz} - \nu\big(\sigma_{xx} + \sigma_{yy}\big)\Big) \quad (16)$$

The overall deformation would be:

$$\varepsilon_{xx} + \varepsilon_{yy} + \varepsilon_{zz} = \frac{1}{E}\big(\sigma_{xx} + \sigma_{yy} + \sigma_{zz}\big)(1 - 2\nu) \quad (17)$$

This equation establishes an upper limit of 0.5 for the value of the Poisson's ratio ν; a material with such property would be incompressible, since the overall deformation would be 0. However, it is important to mention that the above analysis is only valid for isotropic materials, that is, when the values of the elastic constants (in this case, the Young's modulus) are the same in all directions. Table 1-2 lists the Poisson's ratio values for some materials.

Table 1-2: Values of Poisson's ratio for some materials

Material	Poisson's Ratio ν
Aluminum	0.33
Copper	0.36
Lead	0.40 – 0.45
Stainless steel	0.283
Cork	~0.0
Concrete	0.1 – 0.21
Teflon	0.399
Dentine	0.29
Nylon	0.4
Rubber	~0.5

(Gercek, 2007; Solecki and Conant, 2003)

Figure 1.13 shows a solid being deformed by a shear stress. In this case there is only shape change, as shear stresses do not cause normal strains; also, there is no Poisson effect for shear (γ) (Solecki and Conant, 2003).

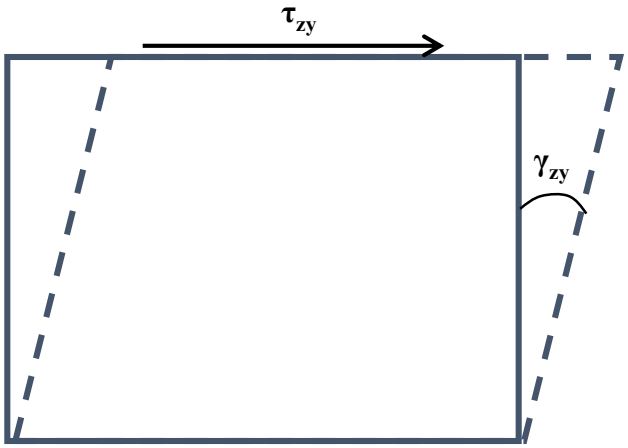

Figure 1.13: Solid under shear stress. Solid lines are the original shape, dashed lines are the deformed shape during application of shear stress.

Similar to the deformation caused by uniaxial stress, the shear strain is related to shear stress by the shear modulus (G). Since there is no Poisson's effect, the equations are much simpler:

$$\gamma_{zy} = \frac{1}{G}\tau_{zy} \quad (18)$$

Similar equations can be established for the other shear strains.

Finally, when a solid is subject to hydrostatic pressure (P), it will undergo change in volume (V). This can be quantified in isotropic materials using a property called bulk modulus (K):

$$\frac{\Delta V}{V} = -\frac{1}{K}\Delta P \quad (19)$$

The inverse of bulk modulus (1/K) is called as compressibility.

Under hydrostatic pressure, the normal stresses have the same magnitude:

$$P = \sigma_{xx} = \sigma_{yy} = \sigma_{zz} \quad (20)$$

Numerically, the value of this hydrostatic pressure is the same as the hydrostatic stress component defined in the previous section.

The values of Young's modulus, Poisson's ratio, shear modulus, and bulk modulus are interrelated in isotropic materials. Once two of these constants are determined, the other two can be calculated using the following equations:

$$G = \frac{E}{2(1+\nu)} \quad (21)$$

$$K = \frac{E}{3(1-2\nu)} \quad (22)$$

(Popov *et al.*, 1976)

According to equation (22), incompressible materials (ν = 0.5), would also have an infinite bulk modulus.

2. Rationale and Hypothesis

2.1. Rationale

A review of some of the literature published on high pressure processing reveals that many researchers accept that pressure is transmitted uniformly across foods during high pressure processing due to the isostatic rule or Pascal's law, even though this law was established for fluids and not for solids. The only work that questioned this principle in high pressure processing was done by Minerich and Labuza (2003). They inserted a copper powder tablet at the center of a ham piece that was later high pressure processed, and by measuring the compression of the tablet they determined that the pressure at the center of the ham was 9 MPa lower than the applied pressure. However, the confidence interval of the correlation between pressure and compression of the sensor was ±16 MPa, so even though the internal pressure was determined to be significantly different from the applied hydrostatic pressure on the surface, the measured difference was within the error of the measurement of an individual sensor. Also, no explanation of why the pressure would decrease from surface to center was provided in this paper. This research was referred by Rastogi *et al.* (2007); curiously in that same review paper the author also stated that pressure is uniform inside food items during HPP, which indicates that the idea of pressure non-uniformity is not accepted by the Food Science community.

2.2. Theoretical Background

From the point of view of solid mechanics, when hydrostatic pressure is applied to a solid material, including food items, the material will compress; the relationship between the applied pressure and the compression of a given material is given by the bulk modulus (see section 1-6). If the food item were composed of two or more materials, each component would be compressed to a different volume depending on their individual bulk modulus. Figure 2.1A represents a simple heterogeneous solid under high pressure, in which the bulk modulus of the inclusion is much higher than the bulk modulus of the soft external material. When pressure is applied, both materials will compress, however the compression of the whole system would not happen as represented in Figure 2.1B. Because of the friction/adherence between the hard inclusion and soft material, the soft material would not slide but instead its boundary region would adhere to the hard inclusion, as shown in Figure 2.1C. Additionally, this friction force at the interface would generate shear stress, since it is a parallel force applied on the boundary surface.

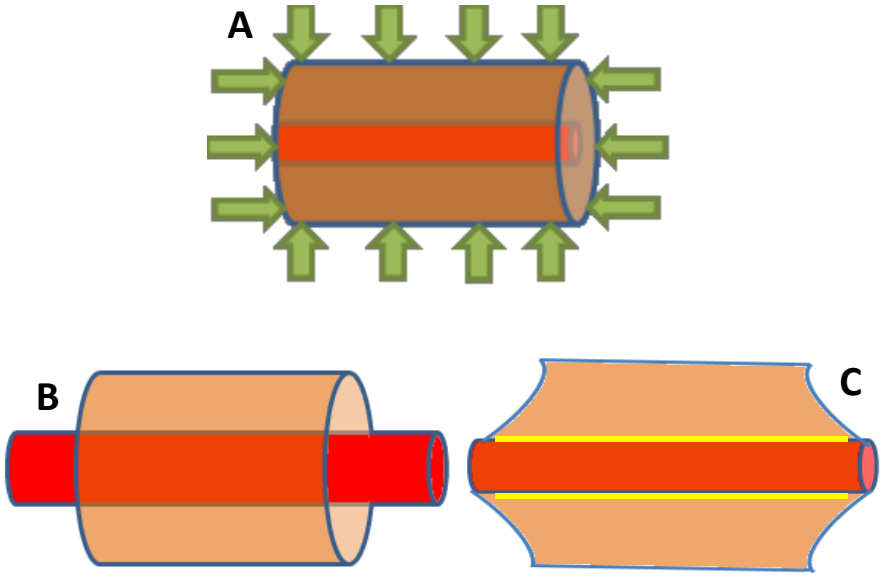

Figure 2.1: (A) Heterogeneous solid under high pressure; (B) independent compression of the materials; and (C) materials bound at the interface

The magnitude of shear stress that develops depends on the difference between the bulk modulus values of the two materials; a higher difference would cause higher difference in the volume compression ($\Delta V/V$ from equation (19)). Because the compression of the soft material at the boundary has to match the compression of the hard material for them to remain attached, this would generate shape change or shear deformation; since the soft material is continuous, this shear deformation in the boundary with the hard inclusion would generate a shear deformation gradient across the whole solid, represented by γ_B at every different position. Using equation (18), the shear deformation would in turn generate shear stress ($\tau_B = G \cdot \gamma_B$).

In order to maintain the strain energy density (which depends on the strain tensor, that includes both pressure and shear strain) constant throughout the material

and comply with law of conservation of energy, the pressure stress needs to decrease accordingly to the generated shear stress, therefore forming a pressure gradient from the surface to the hard inclusion. The decrease in pressure stress needed to accommodate for the generated shear stress depends on the constitutive model of the material; neo-Hookean being one of these models (Bower, 2010).

Numerical simulations of stress distribution for a cylindrical soft material (a 3% agar gel) with a hard inclusion in the central axis when 300 MPa of hydrostatic pressure was applied on the surface were carried out by Dr. Abilash Nair and Dr. Alberto Cuitiño, in the Mechanical and Aerospace Engineering Department, Rutgers University. Figure 2.2 shows the geometry used in the simulations.

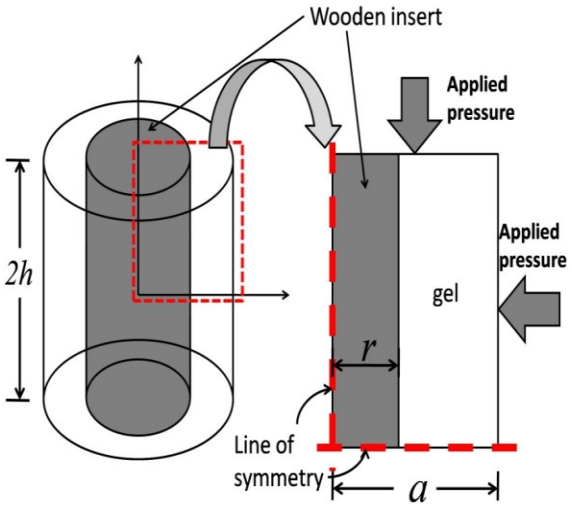

Figure 2.2: Schematic of the two-dimensional axi-symmetric model used for numerical simulation. The vertical dashed line in red is the line of axi-symmetry of the model, while the horizontal red dashed line represents the plane of model symmetry.

The Young's modulus of the hard material was 20 GPa and the Poisson's ratio was 0.3 (Ross, 2010). The compressibility of the soft material was measured using the procedure detailed in section 4.2.d, and additionally different values of Poisson's ratio were considered. The following Neo-Hookean model was used:

$$P = K\frac{\partial U}{\partial J} + \frac{G}{J}\left(\frac{b_{ii}}{3} - 1\right) \quad (23)$$

$$\frac{\partial U}{\partial J} = \frac{lnJ}{J^{3.5}} \quad (24)$$

Where P is the hydrostatic pressure stress, K and G are the bulk modulus and shear modulus of the material (G was calculated from the bulk modulus and Poisson's ratio), b_{ii} is the trace of the left Cauchy-Green tensor ($b_{ii}=\lambda_1^2 + \lambda_2^2 + \lambda_3^2$, where λ is the stretch of the element along the principal axes, that is, the ratio of the length of the deformed element to the length of the un-deformed element along the coordinate system in which the element does not rotate while undergoing deformation), J is the ratio of volume change of the material (ΔV/V), and *∂U/∂J* is a function for the compression of the material, obtained from regression done on the compression data of a 3% agar gel. The K*∂U/∂J* term in eq. (24) represents the volume change and the G/J term the shape change.

As the value of Poisson's ratio ν was decreased from very close to 0.5 and the bulk modulus was kept constant, the Young's modulus and shear modulus increased. Figure 2.3 shows the mesh used to carry out the numerical simulations, obtained from the geometry in Figure 2.2. The stress profiles are shown in Figure 2.4. This means that

bacterial cells located along the radius of the solid would experience different combinations of pressure and shear; depending on how they are affected by each kind of stress, the inactivation values could be non-uniform.

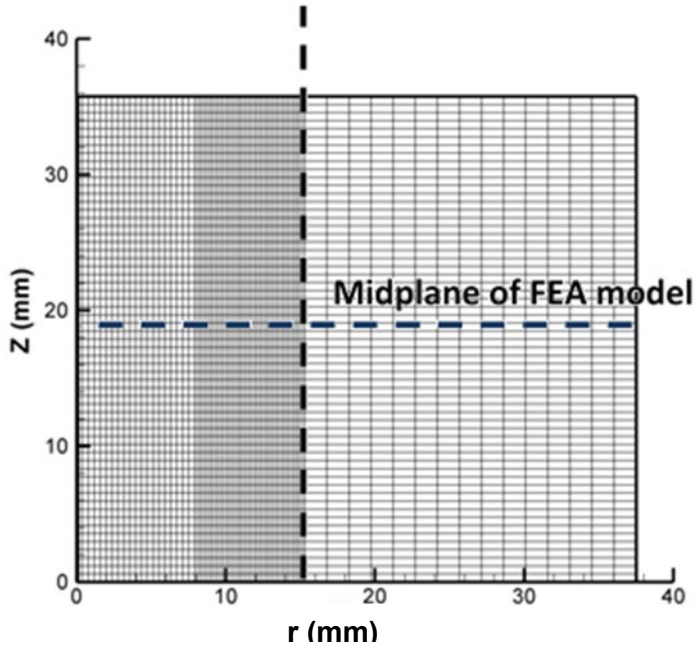

Figure 2.3: Axi-symmetric finite element analysis mesh. The hard insert was between 0 to 8 mm radius (r) and the soft material was between 8 and 38 mm (a=38 mm).

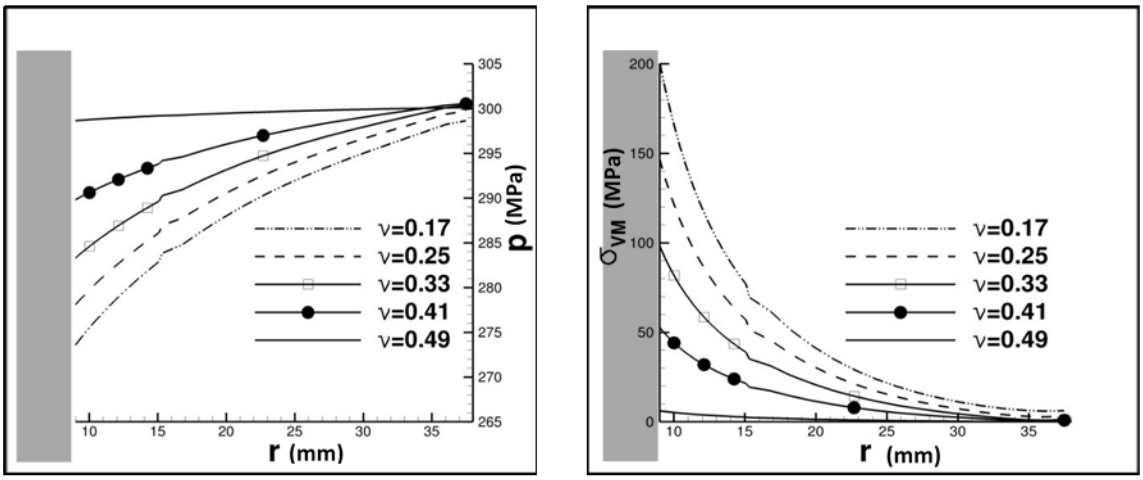

Figure 2.4: Numerical simulation of pressure stress (left) and shear stress (right). The shaded grey region represents the location of the hard inclusion.

Previous research has shown that microbial inactivation is highly sensitivity to the applied hydrostatic pressure (see sections 1-1 and 1-5). However, there is very little research published on the inactivation due to shear stress, especially static shear and at room temperature. Bulut *et al.* (1999), observed a non-trivial effect of shear and thermal forces on the inactivation of *Microbacterium lacticum* during extrusion, and concluded that shear forces played a bigger role in inactivation compared to heat. However, this was for dynamic shear (there is flow during extrusion) and not for static shear, which is the type of shear expected to develop in high pressure processing (where there would not be flow of material). Additionally, Peterson *et al.* (2012) studied the damage of bacterial cells during centrifugation, due to shearing between the cells they had been compacted in a pellet. However, mechanical shear wasn't quantified in this research.

2.3. Hypothesis

A pressure gradient will develop in heterogeneous solid foods during high pressure processing, with the internal pressure being lower than the hydrostatic pressure applied on the surface of the food product. At the same time, a shear stress gradient will develop inside the food item. These two gradients would cause non-uniformity in microbial inactivation.

As established in the previous section, a stress gradient would be established from the surface of the solid to the interface with a hard inclusion, where the hydrostatic pressure component would decrease towards to the inclusion and the shear stress component would increase from the interface. Depending on the location of a microorganism in the solid, it may be subjected to a different combination of pressure and shear stresses. Since pressure stress decreases the volume of a solid maintaining the shape constant and shear stress deforms the solid maintaining the volume constant, it is expected that each will cause failure of the microbial membrane, but not necessarily at the same magnitudes. The combination of the effects may be synergistic or antagonistic. Figure 2.5 shows the effects of pressure stress and shear stress on the geometry of a solid.

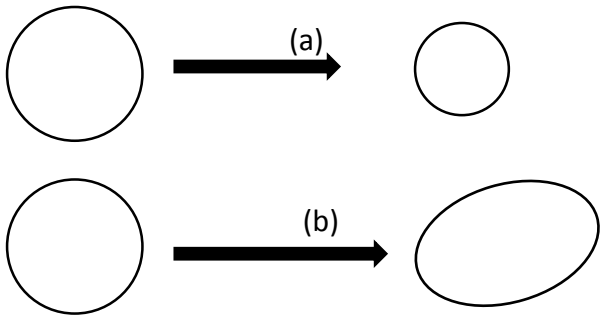

Figure 2.5: Effects of (a) pressure stress, and (b) shear stress on the geometry of a solid

2.4. Objectives

There were two main objectives and two minor objectives in this research project. They were:

1. Quantify the microbial inactivation in different locations in a model system composed of a soft gel with a hard inclusion at the center after high pressure processing.
2. Measure microbial inactivation in model systems with dispersed small hard inclusions after high pressure processing.
3. Design a pressure sensor that could quantify pressure inside solids during high pressure processing.
4. Monitor microbial inactivation in real time during high pressure processing.

Microbial inactivation was used as an indicator of pressure non-uniformity, a difference in inactivation in the model systems could be attributed to the development of stress profiles. Additionally, work was done to use a fluorescence system as a pressure indicator that could potentially be used inside a solid, and this derived into the use of a fluorescent dye to monitor microbial inactivation during high pressure processing.

3. Preliminary Experiments

This chapter briefly covers the experiments done in the early stages of this project, using real food systems (raw chicken drumsticks, raw turkey drumsticks, and smoked turkey drumsticks) to measure microbial inactivation during HPP. It also covers the first model system designed, consisting of an agar, xanthan gum and guar gum gel with a wood inclusion, inoculated in different locations before the gel was fully set. These results were not useful in drawing conclusions for the project.

The experiments with the meat systems gave very inconsistent results, and established the need to use a model system where the geometry and mechanical properties could be kept constant. The first model system designed, where the inoculation was done at specific location, was not the best alternative, as it was difficult to control the exact location of the inoculum. Additionally, it was determined that the attenuated Salmonella strain that was being used was too sensitive to pressure, many of the results with the model system had to be discarded for deviating too much from the rest.

3.1. Materials and Methods

3.1.a. High Pressure Processing Equipment

High pressure processing was carried in a 10 L high pressure vessel (Elmhurst Systems, Albany, NY). Figure 3.1 shows the vessel steel cylinder surrounded by the yolk

that prevents the vessel closure from coming off, as well as the control panel used to program the pressure cycles. Pressurization was achieved with a 20 HP intensifier pump designed to achieve a maximum pressure of 690 MPa, but at the time the project was carried out it wasn't used above 600 MPa. Water at room temperature was used as pressurization medium in all experiments, and temperature never surpassed 40 ºC.

Figure 3.1: 10 L High pressure vessel (steel cylinder) and control panel, at Rutgers University.

3.1.b. Experiments in a Real Food System

An attenuated *Salmonella enterica* strain was grown for 24 h at 37 ºC in trypicase soy broth (Becton, Dickinson and Company, NJ) with 1.5% sodium alginate (KIMICA, Japan). Before using the *Salmonella* suspension, one droplet of food grade color was added, to be able to find the inoculated region afterwards. Food samples of meat with bone, either raw or chicken dumsticks or smoked turkey legs were inoculated by injecting between 0.2 mL to 0.5 mL of culture at different locations relative to the bone (either next to the bone, almost at the surface of the sample, or between the surface and the bone). Immediately afterwards, a volume equal to the inoculum of a 30% $CaCl_2$ solution (Fisher Scientific, NJ) was injected at the same location to gel the *Salmonella* inoculum and prevent it from flowing inside the sample. Figure 3.2 shows a schematic of the inoculation procedure.

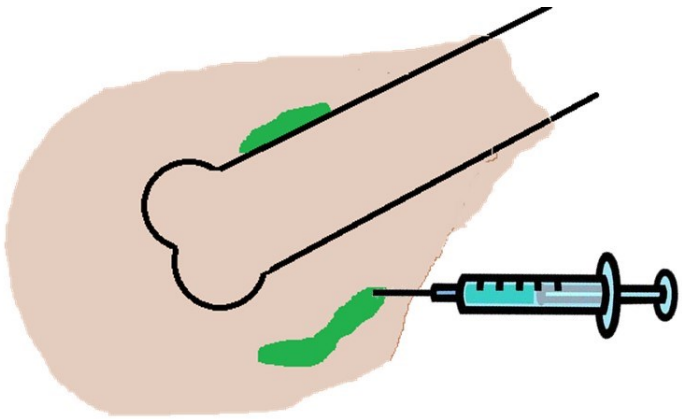

Figure 3.2: Scheme of the inoculation procedure for turkey and chicken drumsticks

The samples were vacuum packed and high pressure processed at 310 MPa or 345 MPa for 5 min. After processing, 10 g of meat containing the inoculum, which was visually identified because of the dye added to the bacterial suspension, was recovered and homogenized with 90 mL of 0.1% peptone water. Plating was done in XLT4 agar (Becton, Dickinson and Company, NJ), plates were left at 37 ºC for 24 h before enumeration. Figure 3.3 shows the recovery of the inoculated meat from a raw chicken drumstick after high pressure processing.

Figure 3.3: Chicken drumstick after HPP. The green regions indicate the Salmonella inoculum

3.1.c. Experiments with a Gel Model System

A model system composed of 1% agar, 0.5% xanthan gum, and 0.5% guar gum (TIC Gums, MD) was formed around a wooden dowel of 1 cm of diameter in a 125 mL plastic bottle, to simulate a drumstick with the bone at the center. The combination of agar, xanthan gum, and guar gum produced a firm but flexible gel, that would have high viscosity when liquid and set relatively quickly as to prevent the spreading of the inoculum.

A small opening was cut out in the bottom at the center of clean polyethylene plastic jars (Fisher Scientific, NJ) of 125 mL capacity. A 1 cm diameter wooden dowel was inserted through the opening. The space between the jar and the dowel was sealed with melted glue. The polymer suspension of 1% agar, 0.5% xanthan gum, and 0.5% guar gum was heated to 90 ºC, cooled down to 40 ºC at room temperature, and then poured into the bottle. Immediately afterwards (before the solid gel was formed), 0.2 mL of colored *Salmonella* suspension (grown in trypticase soy broth, without sodium alginate) was inoculated at different locations using a long pipette tip, according to the diagram in Figure 3.4. The bottles were placed in an ice bath for 15 min for the gel to set quickly so the inoculum stayed in place, and then placed at room temperature to finish setting before high pressure processing.

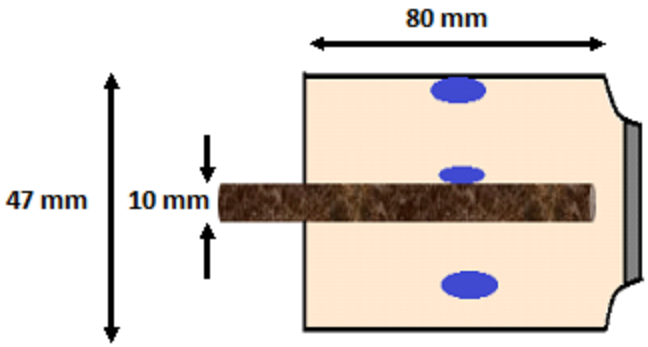

Figure 3.4: Schematic of the first model system. The blue ovals indicate the inoculation locations.

High pressure processing of the model system was carried out at 276 MPa for 3 minutes. Afterwards, 10 g of gel containing the inoculated region were extracted and homogenized in 0.1% peptone water solution. Appropriate dilutions were made before platting in XLT4 media to enumerate the survivors.

3.2. Results and Discussion

Figure 3.5 and Figure 3.6 show the survival of Salmonella at different positions in the turkey drumstick and the model system, respectively, after high pressure processing. Even though there were significant differences observed in the survival of the bacteria, only the difference between the survival at the surface of the gel and at the other two locations was higher than 0.5 log CFU/g. The thickness of the meat was between 20 mm and 50 mm.

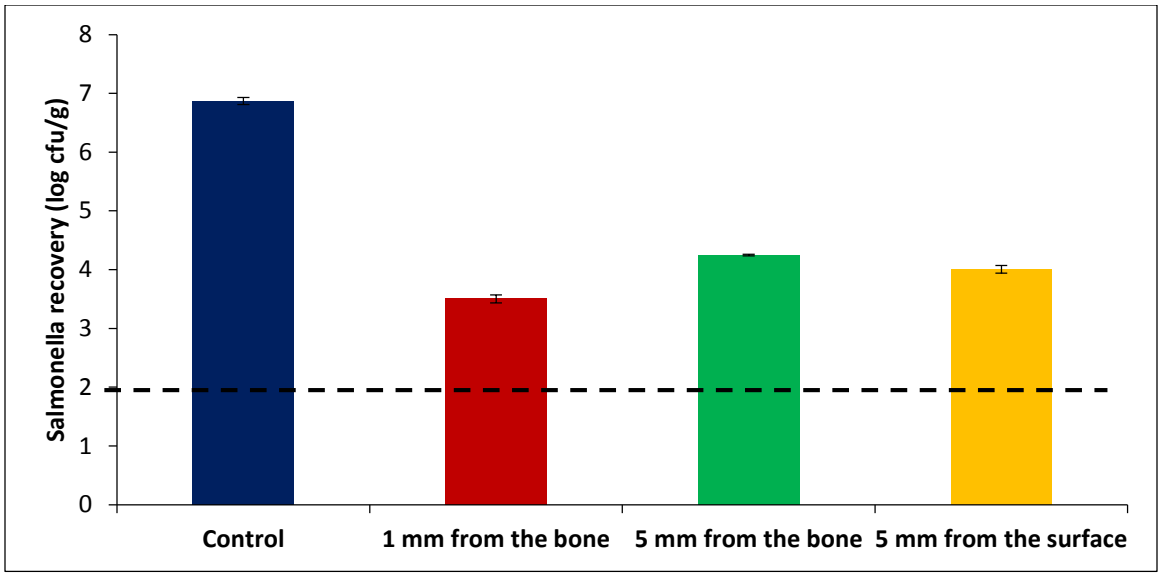

Figure 3.5: Survival of *Salmonella* at different positions in the turkey drumstick after high pressure processing (n=4). The dashed line indicates the limit of detection.

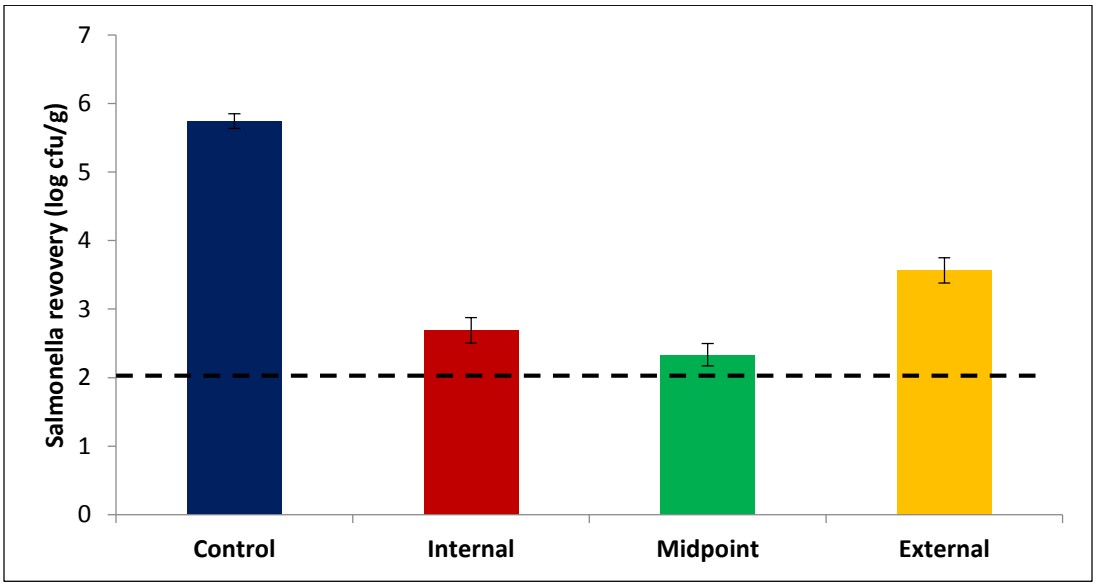

Figure 3.6: Survival of Salmonella at different positions in the gel model system after high pressure processing (n=9). The dotted line indicates the limit of detection.

Many experiments were excluded from these results, and none of the experiments with chicken drumsticks were even included, because the results were very inconsistent. Additionally, the results with the gel model system were too close to the detection limit, which made them unreliable (a small variation in the number of colonies counted would have a big impact on the log cfu/g value). The *Salmonella* strain used was too sensitive to high pressure, so the small variations from one HPP run to another, even at the same conditions, could give highly variable results. It was determined not to work with a real food system (turkey or chicken), and also that the model system had to be redesigned and an organism other than *Salmonella* should be used.

4. Non-Uniformity of Microbial Inactivation in Gel Model Systems during High Pressure Processing

This chapter covers the experiments of microbial inactivation in model systems formulated with a mixture of gelatin and agar or only agar, using a single wood cylinder, or glass wool, or plaster of Paris particles as inclusions. The inclusions were expected to generate different stresses profiles inside the gels. The overall inactivation in the sample was measured in the gels with multiple inclusions, in the gel with one inclusion the inactivation at different positions was measured.

The results showed that the dispersed glass wool or plaster particles affected the microbial inactivation. In the case of *Listeria innocua* (bacteria), the inactivation decreased at increasing amounts of inclusion. In the case of *Saccharomyces cerevisiae* (yeast), the inactivation decreased at lower amounts of inclusions but at higher amounts it was the same as without the inclusions. No inactivation profiles were observed in the system with a single wood inclusion. This very likely implies that non-uniform stress profiles were developed in the regions very close to the inclusions, so the effect on the microbial inactivation was only detected with the glass wool or plaster particles because of the much higher interface area. It also suggests that different organisms react differently to combinations of pressure and shear, and that in the case of yeast, pressure and shear can be antagonistic towards microbial inactivation.

4.1. Literature Review

The only previous work done on pressure non-uniformity during high pressure processing was from Minerich and Labuza (2003). They inserted copper powder tablets in the center of cooked ham, high pressure processed them between 400 MPa and 600 MPa, and measured the compression of the tablets afterwards. The compression of the copper powder tablets was correlated with the applied pressure using the Heckel equation:

$$\ln\left(\frac{1}{\Phi}\right) = KP + A \qquad (25)$$

Where Φ is the material porosity, P is the applied pressure, K and A are constants.

They found that the average calculated pressure inside the ham was 9 MPa lower than the hydrostatic pressure applied on the surface of the hams. Although the average internal pressure was significantly lower ($P<0.017$) than the applied pressure (also quantified using a copper powder tablet), the confidence interval of each individual sensor was ±16 MPa, reducing the reliability of the results. Due to this variability we opted for not using copper powder tables as pressure sensors, besides the fact that we would need to disrupt the solid system in order to insert them.

4.2. Materials and Methods

4.2.a. Microbial Suspension

Listeria innocua ATCC 33090 was grown in BHI broth (BD, MD, USA) with 3% glucose added at 37ºC for 8 h, until it reached approximately 9 log CFU/mL in the early stationary phase. *Saccharomyces cerevisiae* was grown in YPD broth (BD, MD, USA) in agitation at 30ºC for 28 h, until it reached approximately 8 log CFU/mL.

4.2.b. Samples Preparation and Microbial Ennumeration

Gelatin gels were prepared by heating an 18% gelatin 80 bloom (Gelatin Innovations, IL, USA) and 2% agar suspension to 90 ºC. Agar gels were prepared by boiling a 3% agar (RS-100, TIC Gums, MD, USA) suspension. The suspensions were allowed to cool down to 45 ºC before adding 1 mL of microbial suspension per 100 g. A single wood cylinder (obtained from a local hardware store) or glass wool (Corning Inc. Life Sciences, MA, USA) of 8 µm diameter and 2,520 kg/m^3 absolute density were used as inclusions for the gelatin-agar gel, and plaster of Paris (DAP Products, Inc., MD, USA) with 2,690 kg/m^3 absolute density was used as inclusions for the 3% agar gel. Gels without inclusions were also prepared.

After inoculation, the samples were transferred to 125 mL plastic jars and left in the fridge for approximately 36 h before high pressure processing. For the samples that contained a single large inclusion, the wooden cylinder was inserted from the bottom

through the center axis to the jar up to 10 mm before the top. The liquid sample was transferred in and allowed to set around the inclusion. Figure 4.1 shows the design of this model system and the locations where it was sampled after processing; Figure 4.2 shows the model system after being prepared. The gelatin-agar gel with glass wool is shown in Figure 4.3, and the agar gel with plaster of Paris particles is shown in Figure 4.4.

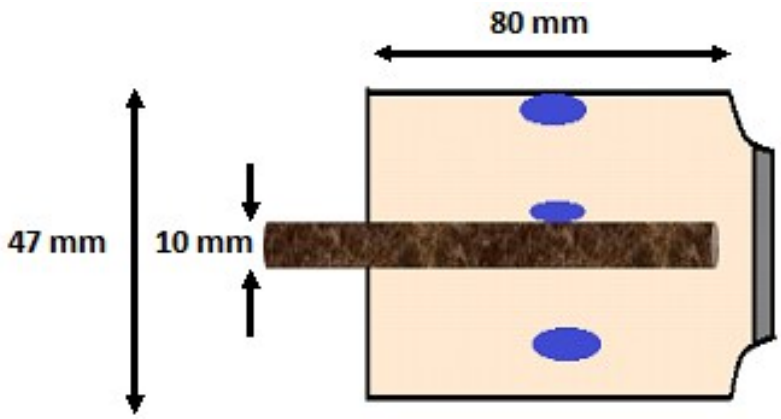

Figure 4.1: Model system of gelatin-agar gel in a bottle around a wood inclusion. The ovals indicate the sampling locations.

Figure 4.2: Gelatin-agar gel model system with a single inclusion, inside the plastic jar (left) and outside the jar (right).

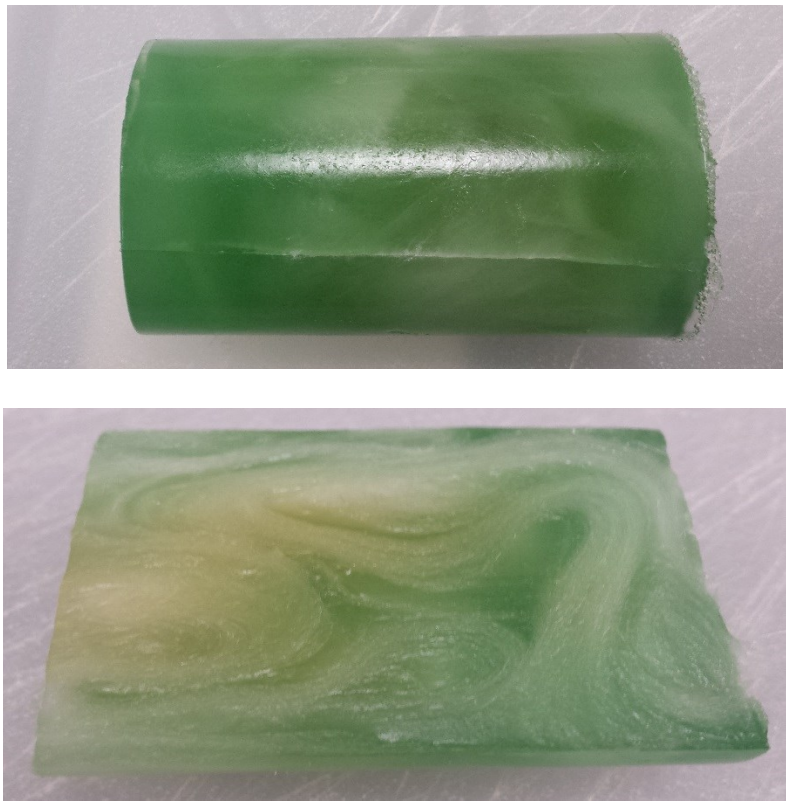

Figure 4.3: Gelatin-agar gel with dispersed glass wool inclusions

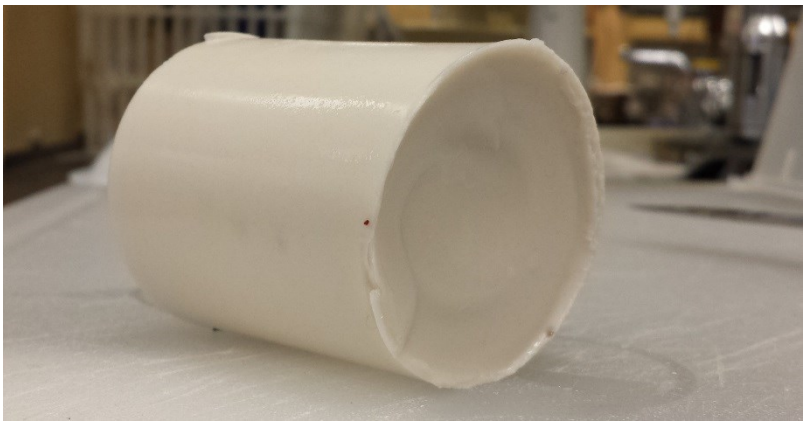

Figure 4.4: Agar gel with dispersed plaster of Paris particles.

Additionally, because plaster of Paris is composed primarily of $CaSO_4$ and calcium had been shown to protect *Listeria innocua* from inactivation due to high pressure processing (Black *et al.*, 2007), the reduction of *Listeria innocua* in water and in 3% agar gel with calcium sulfate dehydrate (Sigma-Aldrich Co. LLC, St. Louis, MO) at its solubility level of 0.24% were also measured. The solubility level was chosen because the protective effect was observed with solubilized calcium ions. Water and agar gels were used to evaluate the independent effects of calcium and if the agar gel matrix would have an additional effect.

Calcium sulfate was added to distilled water and agar suspension. They were boiled and cooled down to 45 ºC before being inoculated with 1 mL of *Listeria innocua* or *Saccharomyces cerevisiae* suspension per 100 mL of water or agar gel. After inoculation, the samples were transferred to 125 mL plastic jars and left in the fridge for approximately 36 h before high pressure processing, similar to the gel samples. Control samples without calcium sulfate were also prepared.

4.2.c. High Pressure Processing

High pressure processing of the gel samples was carried out using the high pressure vessel described in section 3.1.a. Preliminary experiments were carried out to determine a pressure/holding time combination that would achieve partial inactivation of *Listeria innocua* and *Saccharomyces cerevisiae* in the pure 18% gelatin + 2% agar gel model system, so that any potential pressure profiles developed in the samples could be detected by differences in microbial inactivation. The conditions selected were 303 MPa (44 kpsi) for 6 min for *Listeria innocua* and 276 MPa (40 kpsi) for 2 min for *Saccharomyces cerevisiae*.

4.2.d. Microbial Enumeration

After high pressure processing, 1 g of gel were taken from each of the three positions shown in Figure 4.2 of the gelatin-agar gel with a single wood inclusion, and also from an unprocessed gel without an inclusion. The gel samples were transferred to a 7 oz. sterile plastic bag and homogenized by hand-massaging with 9 mL of peptone water. In the case of the gelatin-agar gels with glass wool, 20 g of gel were sampled from the center of the jar and transferred to a large sterile filter bag with 180 mL of peptone water. The samples were homogenized for 4 min using a mechanical stomacher. A similar procedure was followed for the 3% agar gels, with the only difference being that the gels with plaster of Paris inclusions were homogenized with

180 mL of phosphate-buffered saline (PBS; 0.1 M, pH 7.2), which allowed for a higher recovery of *Listeria innocua* cells.

Appropriate dilutions from the homogenates were made using tubes with 9 mL of peptone water. *Listeria innocua* was plated in BHI agar and incubated at 37 ºC for 2 days before enumeration. *Saccharomyces cerevisiae* was plated in YPD agar and incubated at 30 ºC for 3 days before enumeration.

4.2.e. Material Characterization

The bulk modulus of the samples was measured at high pressure, to determine if the overall compressibility of the materials had an effect on microbial inactivation. Measurements were done using a 26 mL tabletop high pressure vessel (Elmhurst Research, Inc., NY, USA). A block of sample, between 8 g to 13 g, was inserted into the vessel and the remaining volume was filled with distilled water. The vessel was pressurized in intervals of approximately 35 MPa (5 kpsi) reaching a maximum pressure of 345 MPa (50 kpsi) using a Carver model K manual press (Carver, Inc., IN, USA). As the pressure increased the piston insertion into the vessel was monitored using an IL-1000 LVDT sensor (Keyence, IL, USA). Figure 4.5 shows the high pressure vessel set up. After each pressurization interval the temperature inside the vessel was allowed to return to its initial value before registering the pressure and the length of the inserted piston. This test was repeated with only distilled water and from the difference between these

experimental results and the NIST data for water density at different pressures a correction factor was calculated to account for compression of seals and other parts inside the vessel.

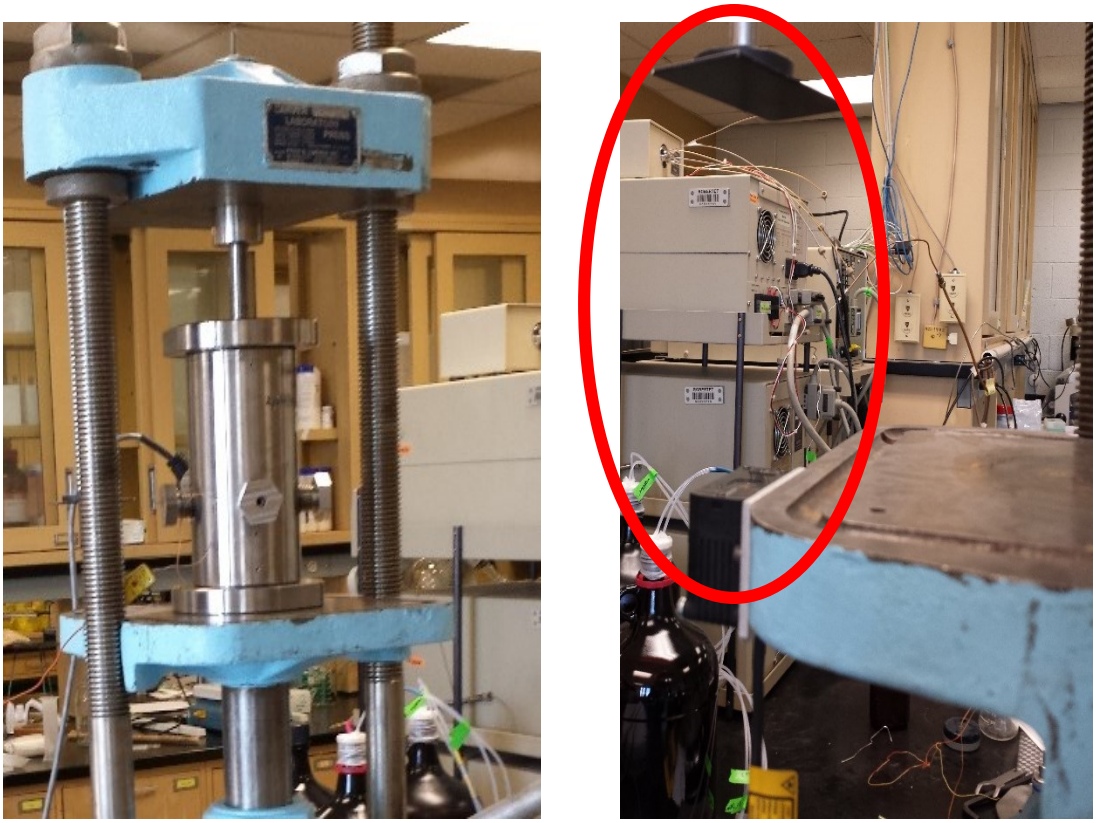

Figure 4.5: 26 mL high pressure vessel on the Carver press (left); detail of the LVDT sensor (right, in the red oval).

Equation (26) was used to calculate the volume of sample at each pressure:

$$V_{S,P} = \left(V_{S,0} + V_{W,0}\right) - \pi \frac{D^2}{4} \Delta h - V_{W,P} - f(P) \qquad (26)$$

Where $V_{S,P}$ is the volume of the sample at each pressure, $V_{S,0}$ is the volume of the sample at atmospheric pressure, $V_{W,0}$ is the volume of the mass of water added at atmospheric pressure, $V_{W,P}$ is the volume of the mass of water added at each pressure

obtained from NIST data (Harvey *et al.*, 2010), *D* is the diameter of the piston, *Δh* is the length of the piston inserted (measured as the change in distance between the LVDT sensor and the platform of the press), and *f(P)* is a volume correction factor obtained from comparing the experimental compression of water and the NIST data.

The correction factor was inserted in equation (26) after observing that the measured values of density of water at high pressure were consistently higher than the values published by NIST. This discrepancy very likely originated from components inside the pressure vessel that were also compressing at high pressure, like seals or the pressure sensor. Since the method used to measure the bulk modulus at high pressure assumes that the volume of inserted piston corresponds to the compression of water and sample, the additional compression of these vessel elements would offset the calculated volumes of the water and sample at high pressure by making them appear to be lower than what they really are. If this calculated volume was then used to calculate the density at high pressure, it would appear to be higher than what it really was. In order to calculate the correction factor, the procedure to measure bulk modulus was followed using only water. Afterwards, the correction factor was calculated by determining what should have been the measured volume at each pressure so the density had matched the one published by NIST. A regression line was obtained in order to determine the correction values to use in the measurements of bulk modulus of the samples. This procedure was followed every day before the measurements of bulk modulus of samples, to account for yielding of the seals.

The bulk modulus (K) was obtained from linear regression between the hydrostatic pressure and the samples volumes, using equation (27):

$$P = K \cdot ln\left(\frac{V_{S,0}}{V_{S,P}}\right) \quad (27)$$

The samples were also observed under an Olympus CX41 (Olympus Corporation, Tokyo, Japan) optical microscope () to determine an approximate size of the plaster of Paris inclusions.

4.2.f. Statistical Analysis

Analysis of variance (ANOVA) was carried out using Excel® 2013 (Microsoft, Redmond, VA) for Windows 64-bits with Daniel's XL Toolbox add-in, version 6.53 (Daniel Kraus, Würzburg, Germany). A significance value of α=0.05 was used for the analysis. Bonferroni-Holm or Student's t-test post hoc tests with α=0.05 were used for paired comparison if ANOVA had shown significant difference between three or more factors. Error bars in the figures represent standard error. Linear regression was also done with Excel 2013.

4.3. Results and Discussion

4.3.a. Material Characterizations

The bulk modulus of the different materials used in the model systems is shown in Figure 4.6. As expected, the materials with lower water content had higher bulk modulus. The gel model system made with 18% gelatin and 2% agar was significantly less compressible than the one made with 3% agar. The addition of glass wool to the gelatin-agar gel model system did not change the overall compressibility of the material. In general, the bulk modulus of the agar gel model system increased with higher volume fractions of plaster of Paris, and the agar gel with 27% (v/v) plaster had similar compressibility as the gelatin-agar gels.

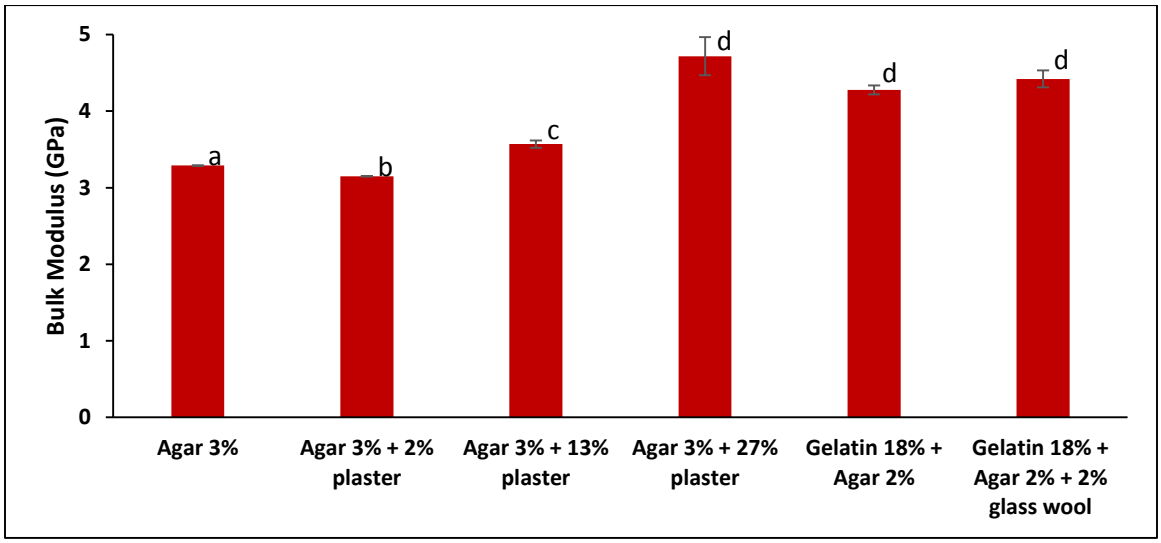

Figure 4.6: Bulk modulus (K) at high pressure of the different materials used in the model systems. Different letter subscripts indicate significant difference (α=0.05) between means using t-test.

A microscope image of the 3% agar gel with 2% (v/v) plaster of Paris is shown in Figure 4.7. The microscope field of view at 100x magnification was determined to be 700 µm, and the size of the observed plaster particles ranged from 4 µm to 40 µm.

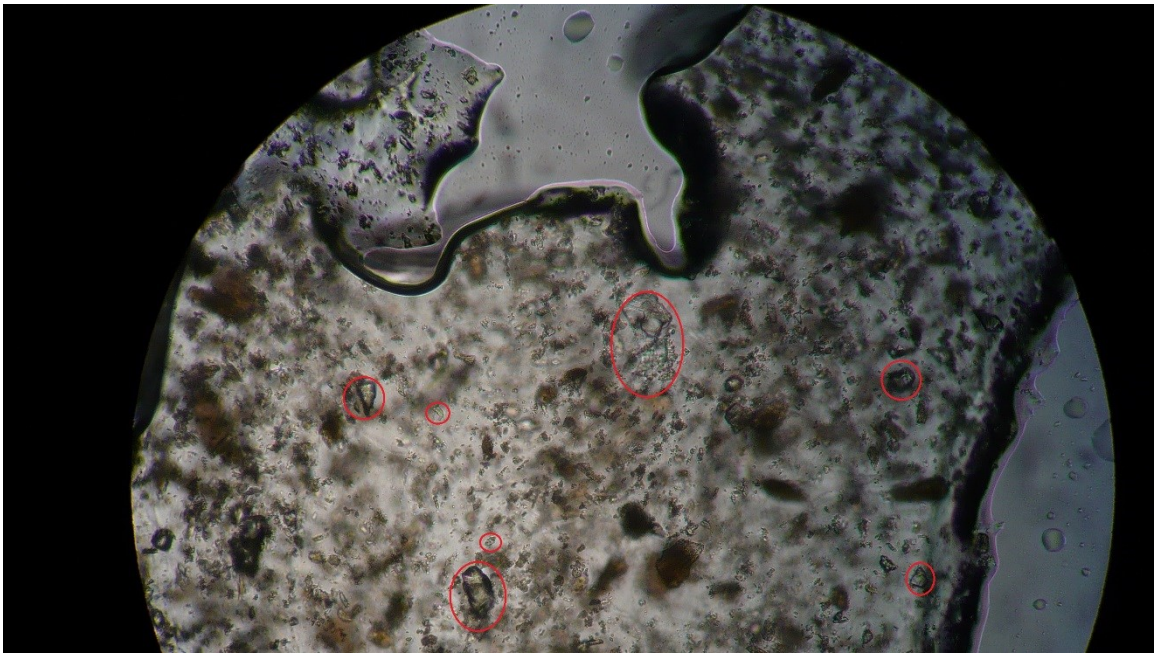

Figure 4.7: Microscope image at 100x magnification of the agar gel + 2% plaster of Paris model system. Circles indicate plaster particles.

4.3.b. Microbial inactivation

The inactivation of *Listeria innocua* after high pressure processing at 303 MPa for 6 min in different locations inside the gelatin-agar with a single wood inclusion model system is shown in Figure 4.8. No significant difference (P=0.46) was found between the three results, as shown in Table 4-1.

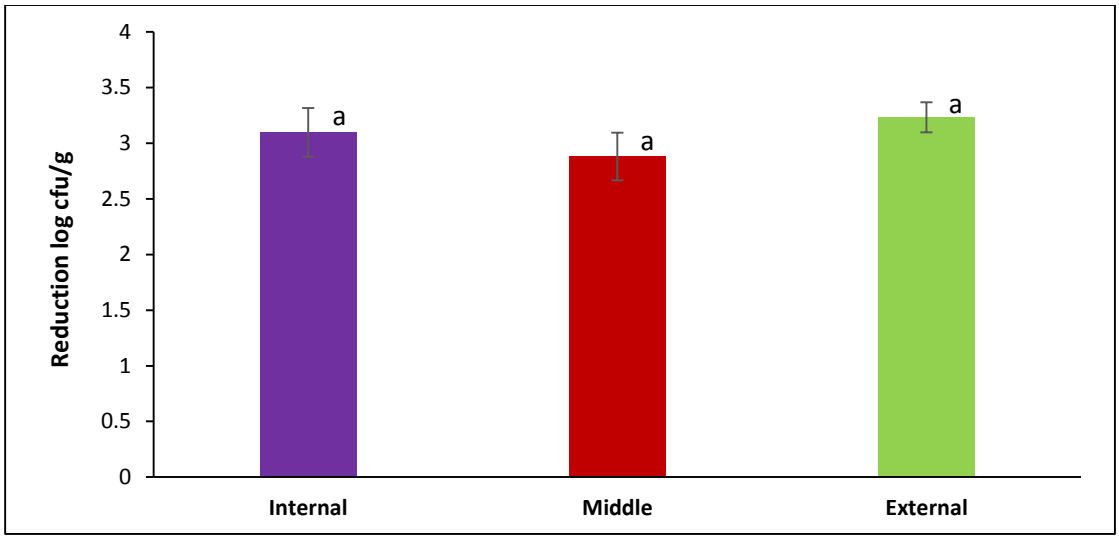

Figure 4.8: Reduction of *Listeria innocua* at different positions in the gelatin-gel with a single wood inclusion model system (n=4).

Table 4-1: ANOVA for reduction of L. innocua at different positions in the model system with one inclusion.

Source of Variation	***SS***	***df***	***MS***	***F***	***P-value***	***F crit***
Between Groups	0.254115	2	0.127058	0.847611	0.459978	4.256495
Within Groups	1.349108	9	0.149901			
Total	1.603223	11				

The inactivation of *Listeria innocua* and *Saccharomyces cerevisiae* inside the gelatin-agar model system with glass wool inclusions after high pressure processing at

303 MPa (44 kpsi) for 6 min and 276 MPa (40 kpsi) for 2 min, respectively, are shown in Figure 4.9. Unlike the previous experiment, the hard inclusions (glass wool fibers) were dispersed all over the gel, so the gels were sampled only once and at the center. The glass wool caused a significantly lower (α=0.05) inactivation level for both organisms compared to the sample without the inclusions. The ANOVA results are in Table 4-2 and Table 4-3, and the results of the Bonferroni-Holm post-hoc test (α=0.05) are in the letter subscripts in Figure 4.9. The experiment with glass wool at 6% (v/v) was only repeated twice and only with *Listeria innocua*, due to the difficulties in pouring the melted gel in the void space left by the glass wool in the plastic jar. Because of this limitation, the model system of agar gel with plaster of Paris particles was designed.

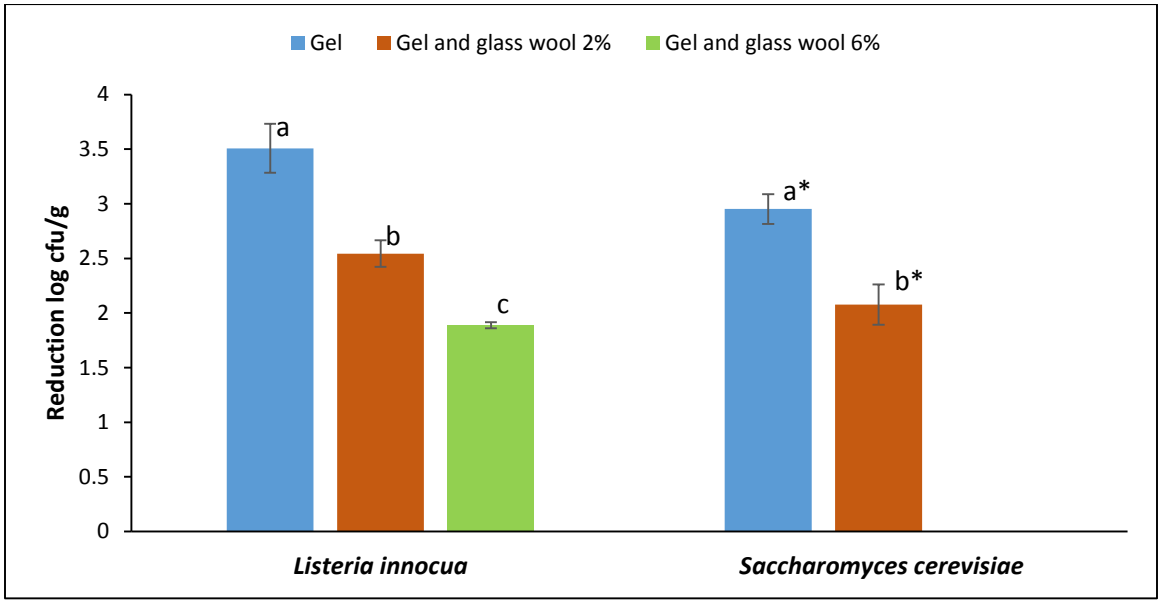

Figure 4.9: Microbial reduction in the model system of gelatin-agar gel with glass wool fibers (n=4). Statistical analysis done between results for the same organism.

Table 4-2: ANOVA of reduction of *Listeria innocua* in the gelatin-agar gel with glass wool model system.

Source of Variation	***SS***	***df***	***MS***	***F***	***P-value***	***F crit***
Between Groups	4.389644	2	2.194822	14.88451	0.002013	4.45897
Within Groups	1.179655	8	0.147457			
Total	5.569299	10				

Table 4-3: ANOVA of reduction of *Saccharomyces cerevisiae* in the gelatin-agar gel with glass wool model system.

Source of Variation	***SS***	***df***	***MS***	***F***	***P-value***	***F crit***
Between Groups	1.529433	1	1.529433	14.44305	0.008964	5.987378
Within Groups	0.635364	6	0.105894			
Total	2.164798	7				

The 3% (w/w) agar gel was able to hold in suspension between 2% (v/v) and 27% (v/v) of plaster of Paris particles. The results of *Listeria innocua* and *Saccharomyces cerevisiae* reduction after HPP treatments similar as above (303 MPa x 6 min for *Listeria* and 276 MPa x 2 min for Saccharomyces) are shown in Figure 4.10. A significantly lower (α=0.05) inactivation was observed in the gel with 2% plaster compared to the gel without inclusions; a similar trend as with the glass wool inclusions. In the case of *Listeria innocua*, the inactivation significantly decreased (α=0.05) with 13% and 27% of

plaster compared to 2% plaster (however, no significant difference was observed between the two samples with higher amount of plaster). In the case of *Saccharomyces cerevisiae*, the inactivation in the samples with 13% and 27% of plaster returned to the levels of the sample without inclusion, no significant difference (α=0.05) between them was observed. The results of ANOVA are shown in Table 4-4 and Table 4-5, and the results of the Bonferroni-Holm post-hoc test (α=0.05) are in the letter subscripts in Figure 4.10.

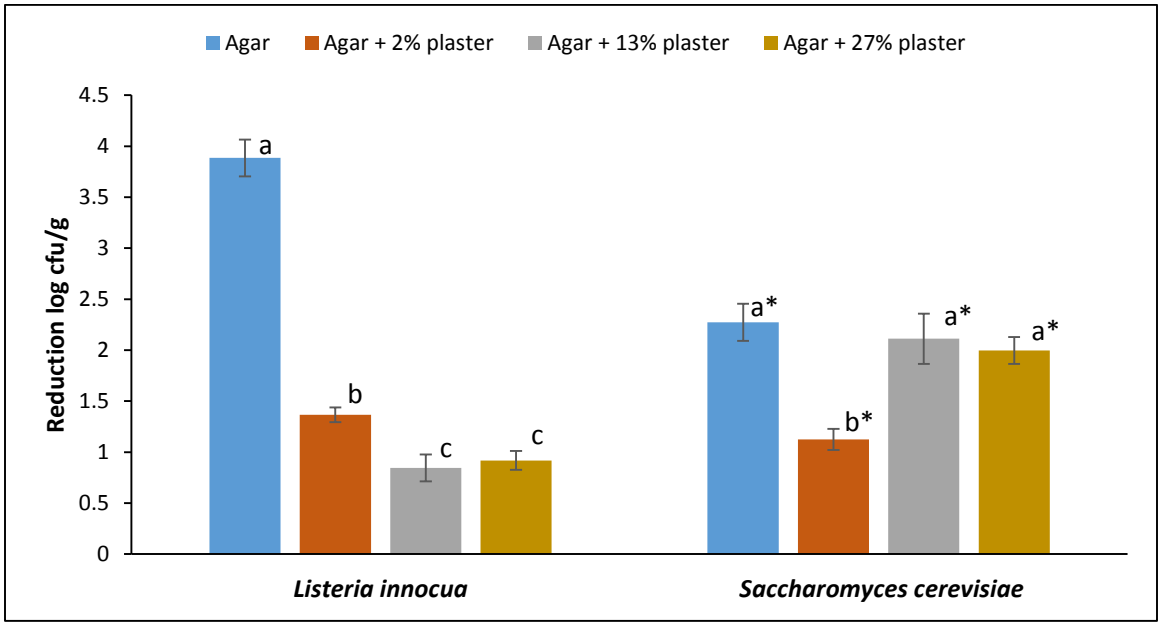

Figure 4.10: Microbial reduction in the model system of agar gel with plaster particles (Listeria: n=4, Saccharomyces: n=7). Statistical analysis done between results for the same organism.

Table 4-4: ANOVA of *Listeria innocua* reduction in agar gel with plaster particles model system.

Source of Variation	***SS***	***df***	***MS***	***F***	***P-value***	***F crit***
Between Groups	37.11071	3	12.37024	104.958	7.81E-10	3.343889
Within Groups	1.650024	14	0.117859			
Total	38.76073	17				

Table 4-5: ANOVA of *Saccharomyces cerevisiae* reduction in agar gel with plaster particles model system.

Source of Variation	***SS***	***df***	***MS***	***F***	***P-value***	***F crit***
Between Groups	5.008844	3	1.669615	8.48137	0.000696	3.072467
Within Groups	4.133992	21	0.196857			
Total	9.142836	24				

The effects of $CaSO_4$ on the reduction of *Listeria innocua* after high pressure processing (303 MPa x 6 min, same conditions as the previous experiments) are shown in Figure 4.11. A significantly lower inactivation (α=0.05) was observed in water with 0.24% $CaSO_4$ compared to pure water, however no difference was observed in the agar gel with and without $CaSO_4$. The results of the ANOVA are shown in Table 4-6, and and the results of the Bonferroni-Holm post-hoc test (α=0.05) are in the letter subscripts in Figure 4.11.

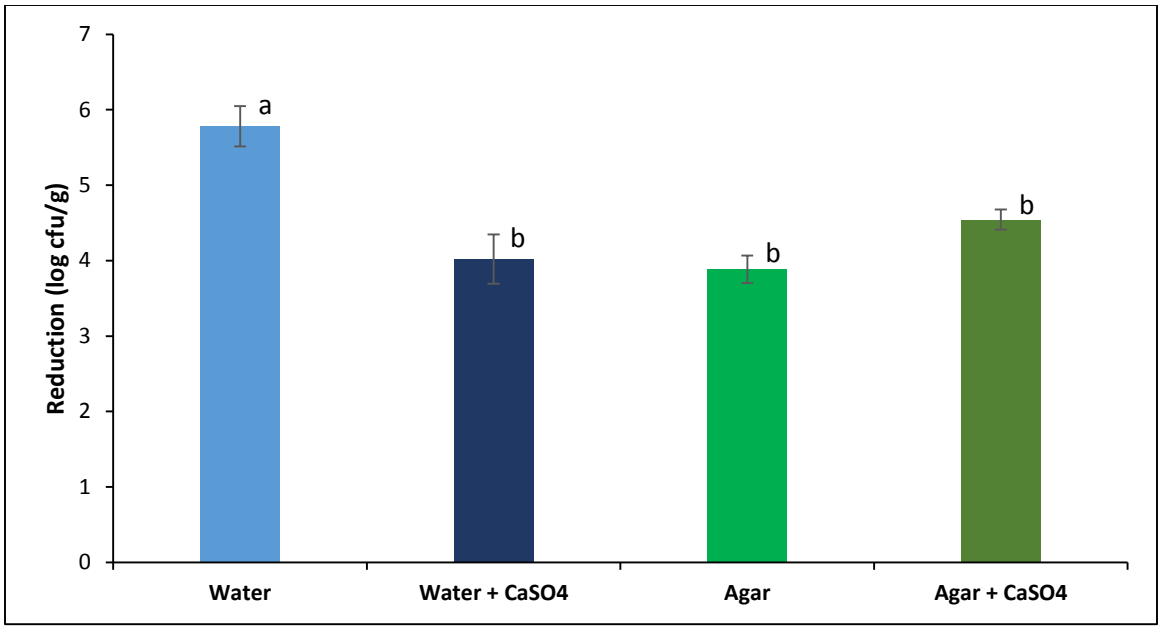

Figure 4.11: Reduction of *Listeria innocua* after high pressure processing in water and agar gel with calcium sulfate (n=4 for water, n=7 for water + $CaSO_4$ and agar, n=4 for agar + $CaSO_4$).

Table 4-6: ANOVA of *Listeria innocua* reduction in water and agar gels with $CaSO_4$.

Source of Variation	***SS***	***df***	***MS***	***F***	***P-value***	***F crit***
Between Groups	17.11073	3	5.703578	12.5137	5.51E-05	3.049125
Within Groups	10.02731	22	0.455787			
Total	27.13804	25				

Comparing the bulk modulus of the model system materials (Figure 4.6) with the achieved microbial inactivation (Figure 4.9 and Figure 4.10), we can infer that the overall compressibility of the materials did not influence microbial inactivation. For example, no significant difference was found in the bulk modulus of the gelatin gel with and without

glass wool fibers, however the inactivation of *Listeria innocua* and *Saccharomyces cerevisiae* was significantly difference between those two materials (α=0.05). Additionally, no significant difference was observed between the inactivation of *Listeria innocua* in the gelatin-agar gel and agar gel without inclusions (P=0.216, from a t-test), although the bulk modulus of the materials were significantly different. In the case of *Sacharomyces cerevisiae*, a significant difference was observed between the inactivation in the above materials, but the probability value was on the high end (P=0.024).

The results shown in Figure 4.8 would indicate that no stress profile was established in the model system during high pressure processing, given that there was no difference in the inactivation at different distances from the hard inclusion at the center. However, it is possible that the stress profile only formed in regions very close to the inclusion, and that even the cells from the location sampled close to the inclusion were too far away from it (bacteria cells are approximately 1.5 µm in diameter, if the samples location was an average of 5 mm away from the inclusion, that would still be 3 orders of magnitude larger, an equivalent to 1 Km in human perspective). The results from the gel with glass wool model system support this idea, as both *Listeria innocua* and *Saccharomyces cerevisiae* had significantly lower inactivation when 2% (v/v) glass wool were added to the gel (Figure 4.9). By replacing the single 10 mm diameter wood inclusion with 2% (v/v) of 8 µm diameter glass wool fibers, the interface area increased 500 times, so the effect of cells surviving when located very close to the hard inclusions was detectable.

The results with the agar gel with plaster particles model system also supported the idea that a stress profile formed very close to the inclusions. Using plaster of Paris particles allowed a wide range of volume fraction of hard inclusions in the gel. In the case of *Listeria innocua*, as the volume of plaster increased from 0% to 2%, and to 13% and 27%, the inactivation decreased (Figure 4.10). No significant difference in the inactivation was found between 13% and 27% plaster, likely because doubling the amount of particles didn´t make a difference detectable in the log scale used to quantify the surviving microorganisms. In case of *Saccharomyces cerevisiae*, also shown in Figure 4.10, the microbial reduction significantly decreased between 0% and 2% of plaster, but it went back up to values similar to the gel without inclusions when 13% and 27% were added.

Based on the results from the numerical simulation of stress distribution in a soft material with one inclusion, shown in Figure 2.4, in the regions close to the inclusions the hydrostatic pressure stress would be at its minimum and shear stress would form. In the regions further away from the inclusions the pressure stress should increase and the shear stress would decrease, and even further away the pressure stress would be almost equal to the applied hydrostatic pressure and the shear stress would be almost zero. In the model system of agar gel with plaster, when the amount of plaster particles was increased to 13% and 27% it is very likely that the regions on high shear – low pressure were increased, compared to the agar gel with 2% plaster where the regions of medium shear – medium pressure should have been more prevalent.

Depending on the susceptibility of a specific organism to pressure or shear, or to their interaction, the effect on inactivation would be different. The inactivation of *Listeria innocua* decreased upon increase of the number of inclusions, both glass wool fiber and plaster particles, so it is likely that the cell wasn't affected by the shear stress formed around the inclusions. In the case of *Saccharomyces cerevisiae*, it is likely that the combination of pressure and shear was antagonistic for microbial inactivation, so reduction was at its lowest with 2% plaster. When the amount of plaster increased and more yeast cells were exposed to higher shear stress and lower pressure, the average inactivation was similar as the material without any inclusions.

Buckling is a phenomenon that takes place, among many scenarios, in thin shells under load (Tasi, 1966; Seaman, 1962), and it is expected that it would happen with microbial cells under high pressure. The Young's modulus of *Saccharomyces cerevisiae* cell wall has been measured and models have been developed and validated with the assumption that it is incompressible (Stenson *et al.*, 2011; Stenson *et al.*, 2009; Smith *et al.*, 2000a; Smith *et al.*, 2000b). Assuming a Young's modulus of 112 MPa, the lowest value indicated by these authors, and a Poisson's ratio of 0.499, consistent with the assumption of an incompressible material, the bulk modulus of the yeast cell wall would be 18.7 GPa according to equation (22). Since the cell cytoplasm main component is water, its bulk modulus would be close to 3.3 GPa (calculated using NIST data for water a high pressure). Given the differences in compressibility between the yeast cell wall and cytoplasm, it is very likely that the yeasts buckle during high pressure

processing. Additionally, buckling has already been observed in carrot cells after 300 MPa for 2 min (Trejo Araya *et al.*, 2007).

The development of shear stress in addition to pressure would reduce buckling. Figure 4.12 shows the different scenarios of yeast cell compression and deformation during high pressure processing. If no buckling would take place, the cell wall and cytoplasm would separate, so that scenario is not possible. If only pressure was applied the cell wall would need to buckle and loose its globular shape so the internal surface area of the cell wall matches the surface area of the cytoplasm while maintaining the volume reductions due to pressure. If shear was applied in addition to pressure, the cell would lose its globular shape due to shear deformation and the need to buckle so the internal cell wall surface and cytoplasm surface match would be less.

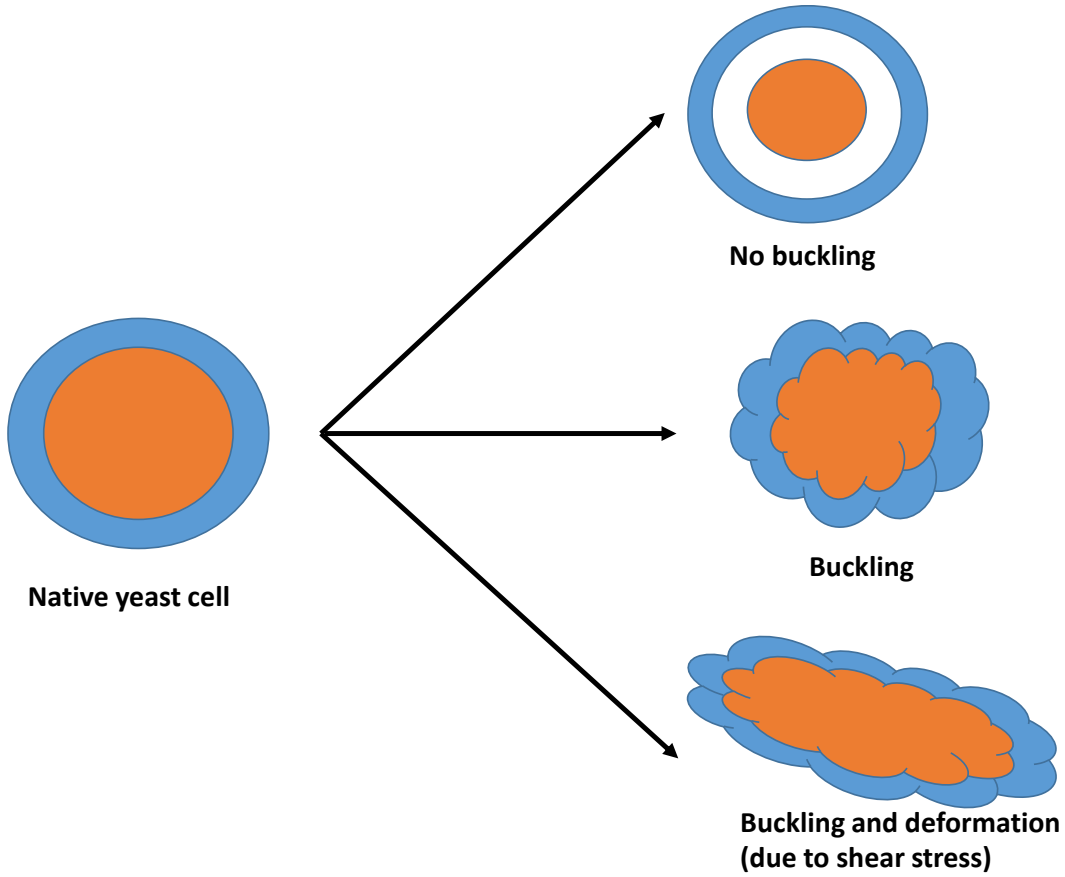

Figure 4.12: Schematic of the possible yeast cell compression and deformation scenarios during high pressure processing.

Therefore, if buckling was involved in the inactivation by cell wall rupture of *Saccharomyces cerevisiae* cells during high pressure processing, very possible given that the models developed by Huang *et al.* (2008) predicted the development of cracks around local deformations in the cell wall of *E. coli*, the development of shear stress in the vicinity of the plaster particles would reduce it. This would explain why the reduction in the model system with only 2% plaster particles was the lowest. When the amount of plaster particles increased, the effects of the high shear – low pressure developed next to the plaster particles could have damaged the cell wall of the yeasts

but in a different way and increased the microbial inactivation. The absence of this effect on *Listeria innocua* could be explained because it is natively further away from being sphere-like (*Listeria* is a rod-shaped organism), so the effect of cell wall buckling should have a lower participation on overall inactivation.

5. Development of a Fluorescent Pressure Sensor and In situ Studies of Microbial Inactivation during High Pressure Processing

This chapter describes the experiments aiming to develop a pressure sensor based on the increase of Förster resonance energy transfer (FRET) between two chromophores as they get closer due to the compression caused by the pressure. Additionally, it includes the work done to obtain real-time data of microbial inactivation during high pressure processing. In both cases the experiments were done in the small tabletop high pressure vessel, which had sapphire windows that allowed to make spectrophotometric measurements during processing.

The FRET pair chosen was Nile red and diphenylhexatriene (DPH), which has been shown to give fluorescence in an aqueous solution with lipid particles. Unfortunately no emission from Nile red was detected upon excitation of the DPH at 390 nm, so the experiment was unsuccessful. The microbial inactivation was monitored through propidium iodide fluorescence, using *Enterobacter aerogenes*. We were able to determine that no appreciable inactivation happened during depressurization, and that it is likely that reversible disassociation of ribosomes took place inside the cells after the cell membrane was compromised due to pressure.

5.1. Literature Review

5.1.a. Mechanism of Förster Resonance Energy Transfer (FRET)

FRET involves the non-radiative transfer of energy from an excited chromophore (called donor) to another chromophore (called acceptor) by long-range dipole-dipole coupling (Clegg, 1995; Förster, 1948). The efficiency of energy transfer (E) is given by:

$$E = \frac{1}{1+\left(\frac{R}{R_0}\right)^6} \qquad (28)$$

where R is the distance between the acceptor and donor molecules pair, and R_0 is the distance at which 50% of the energy is transferred (constant for the pair). The transfer results in a decrease in the fluorescence emission of the donor and an increase in the fluorescence emission of the acceptor, which are used to determine *E*, which in turn can be used to measure *R* (Ha, 2001). Wu and Brand (1994) compiled a list of 70 FRET pairs with their R_0 value.

FRET is widely used in the study of biological systems, some of the applications include DNA rulers, staphylococcal nuclease, biotin-streptavidin, GCN4 peptides, α-tropomyosin, S15 binding RNA junction, Tetrahymena ribozyme, calmodulin, and Rep helicase (Ha, 2001).

5.1.b. Use of Fluorescent Dyes in Cell Inactivation Studies

Fluorescent dyes, propidium iodide among them, have been extensively used as fast methods to measure microbial inactivation using flow cytometry. Propidium iodide penetrates unviable cells with damaged or permeabilized membrane (Boulos *et al.*, 1999; Nebe-von Caron *et al.*, 1998) and binds to nucleic acids (DNA or RNA) increasing its fluorescence signal 20 or 30 times, with an emission peak at around 620 nm (invitrogen, 2006). Propidium iodide has been used to study the relationship between membrane fluidity and inactivation due to HPP in *Lactobacillus plantarum* (Smelt *et al.*, 1994), to assess the inactivation in different strains of *E. coli* 0157 due to HPP (Benito *et al.*, 1999), and to study the membrane rupturing in *Listeria monocytogenes* after HPP (Ritz *et al.*, 2001). It was also used to conclude that pressure inactivation was mostly due to membrane damage but thermal inactivation was not necessarily due to it in *Lactobacillus rhamnosus* (Ananta and Knorr, 2009). Additionally, it was used to assess membrane integrity of mammalian skeletal muscle fibers during high pressure treatment using in-situ fluorescence microscopy (Friedrich *et al.*, 2006).

5.2. Materials and Methods

5.2.a. High Pressure Processing

A 26 mL capacity tabletop high pressure vessel (Elmhurst Research, Albany, NY), that can reach a maximum pressure of 800 MPa. The vessel has three sapphire windows

with non-reflective coating (Kyocera Industrial Ceramics Corp., Kyoto, Japan) of 10 mm diameter and 12.5 mm length, which allow for optical access for excitation and fluorescence emission through fiber optic probes. The vessel was pressurized by inserting a piston, using a manual model K (Carver, Wabash, IN) hydraulic press. The pressurization rate was approximately 103 MPa/min (15 kpsi/min). Fluorescence was measured with a SILVER-Nova 200 TEC BW16 (StellarNet, Inc., Tampa, FL) spectrometer with 10,000 ms integration time (the accumulation time of light input before the spectrometer provided the spectrum output). Excitation was done with a SL-1 (StellarNet, Inc., Tampa, FL) LED lamp. Figure 5.1 shows the high pressure vessel on the press, with the spectrometer and LED lamp connected to the sapphire windows through optical fiber cables. Figure 5.2 shows a schematic of the sapphire windows in the high pressure vessel.

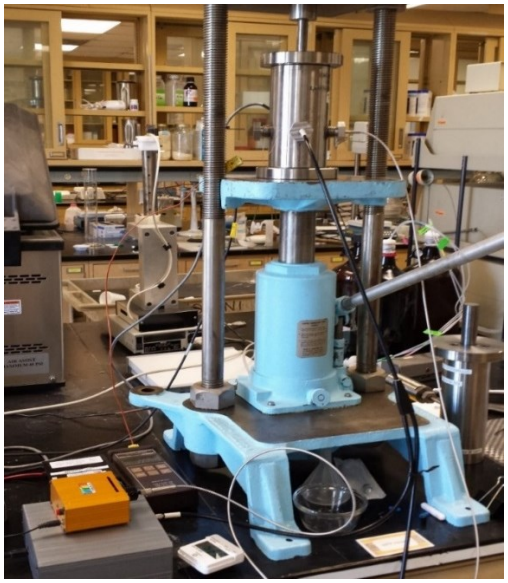

Figure 5.1: Tabletop high pressure system, with spectrometer and LED lamp (bottom left).

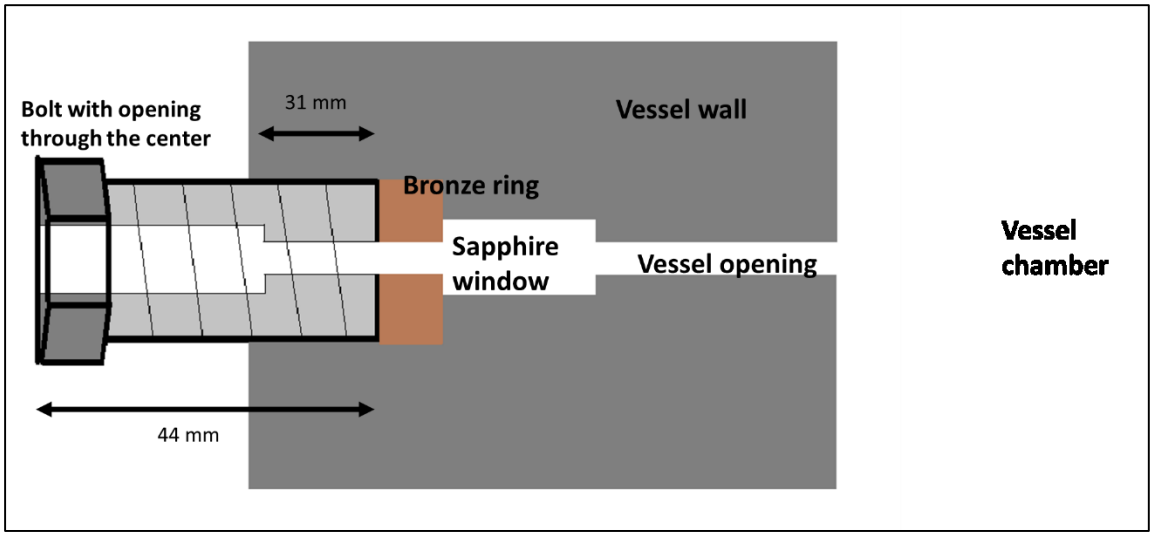

Figure 5.2: Schematic of sapphire windows in high pressure vessel (not on scale).

5.2.b. Development of a Pressure Sensor

The FRET system studied by Jain and Das (2006), using Nile red and diphenylhexatriene (DPH) as acceptor and donor, respectively, in a lipid environment was adapted. Upon compression of the system due to hydrostatic pressure, it was expected that the average distance between the donor and acceptor would be reduced and therefore the energy transfer after excitation of the donor would increase, as pointed out in equation 26.

The lipid system was formed by homogenizing a 2% mineral oil (Foodtown, NJ) and 0.1% sodium lauryl sulfate (Spectrum Chemical MFG Corp, New Brunswick, NJ) using a Polytron PT 1600E (Kinematica, Schweiz, Switzerland) high shear homogenizer for 1

min at 10,000 RPM. The FRET system was formed with 4 µM of Nile red and 4 µM of DPH, using stock solutions of 1 mM Nile red in methanol and 500 µM DPH in tetrahydrofuran. Pressurization was done from atmospheric pressure to 172 MPa (25 kpsi). Emission spectrum was recorded on intervals of 34 MPa (5 kpsi). Excitation of DPH was done at 390 nm.

Additionally, fluorescence of Nile red alone in the lipid system was measured, to be able to account for the effects of the increase in dye concentration due to compression during pressurization. Concentrations from 1.2 µM to 7.2 µM were tested. Excitation of Nile red was done at 545 nm.

Finally, the effects of pressurization on fluorescence of Nile red were measured using 4 µM of Nile red and 12 µM of DPH in the lipid system, which was pressurized up to 276 MPa (40 kpsi). Excitation of Nile red was done at 545 nm.

5.2.c. In situ Studies of Microbial Inactivation during HPP

Nalidixic acid-resistant *Enterobacter aerogenes* (Gram negative bacteria) was grown in 25 mL of trypticase soy broth (Becton, Dickinson and Company, NJ, USA) with 50 mg/L of nalidixic acid, for approximately 20 h at 37 ºC, which assured the cells were in stationary phase. The cultures were centrifuged at 6,000 x g for 10 min in a Sorvall Legend X1R (ThermoFisher Scientific, Waltham, MA) and the supernatant replaced with phosphate-buffered saline (PBS; 0.1 M, pH 7.2). After washing, the suspension

contained approximately 8.5 log cfu/mL of viable bacteria. 15 µg/mL of propidium iodide was added to the *Enterobacter aerogenes* suspension prior to HPP, using a 500 µg/mL stock solution previously prepared and kept under refrigeration and protected from the light. Enumeration after processing was done in trypticase soy agar (Becton, Dickinson and Company, NJ, USA) with 50 mg/L of nalidixic acid; the suspensions used for enumeration did not have propidium iodide added.

Additionally, *Listeria innocua* ATCC 3390 and *Saccharomyces cerevisiae* were grown in BHI broth for 20 h at 37 ºC and YPD broth for 28 h at 37 ºC under agitation, respectively, and washed at 6,000 x g for 10 min or 1,500 x g for 2 min and suspended in PBS. 15 µg/mL of propidium iodide was also added before HPP.

Three different pressurization processes were applied. The first process had 3 min cycles at 207 MPa, 267 MPa and 345 MPa with 2 min holding at atmospheric pressure between cycles. The second had 45 s and 4 min cycles at 267 MPa and a cycle at 207 MPa for 2 min with 2 min holding at atmospheric pressure between cycles. The third process had a cycle of 7 min at 207 MPa directly followed by 6 min at 267 MPa. Excitation was done at 490 nm and fluorescence emission was monitored at 622 nm.

5.3. Results and Discussion

5.3.a. Development of a Pressure Sensor

Fluorescence was not detected from the FRET system when excited at 390 nm, at atmospheric pressure or at high pressure. The most likely reason was that the energy transfer between DPH and Nile red was too small, which in turn caused a very weak emission from Nile red which wasn't detectable by our set up. Due to the thickness of the pressure vessel (see Figure 5.2) and the small size of the fiber optic probe (5 mm in diameter), only a very small fraction of the light from inside the vessel would be able to escape and be transferred to the sprectrophotometer.

Nile red produced fluorescence when excited at 545 nm, both at atmospheric pressure and at high pressure. Figure 5.3 shows the fluorescence spectrum of different concentrations of Nile red at atmospheric pressure, with peak emission at 643 nm. The emission intensities are plotted in Figure 5.4, showing a linear correlation between emission and concentration.

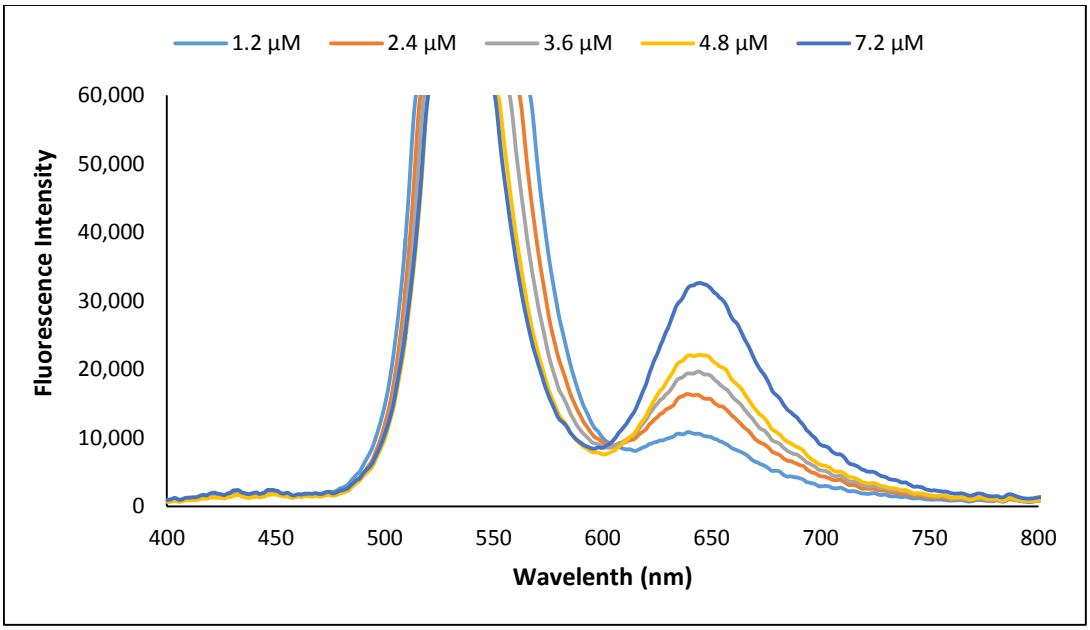

Figure 5.3: Spectrum of different concentrations of Nile red at atmospheric pressure.

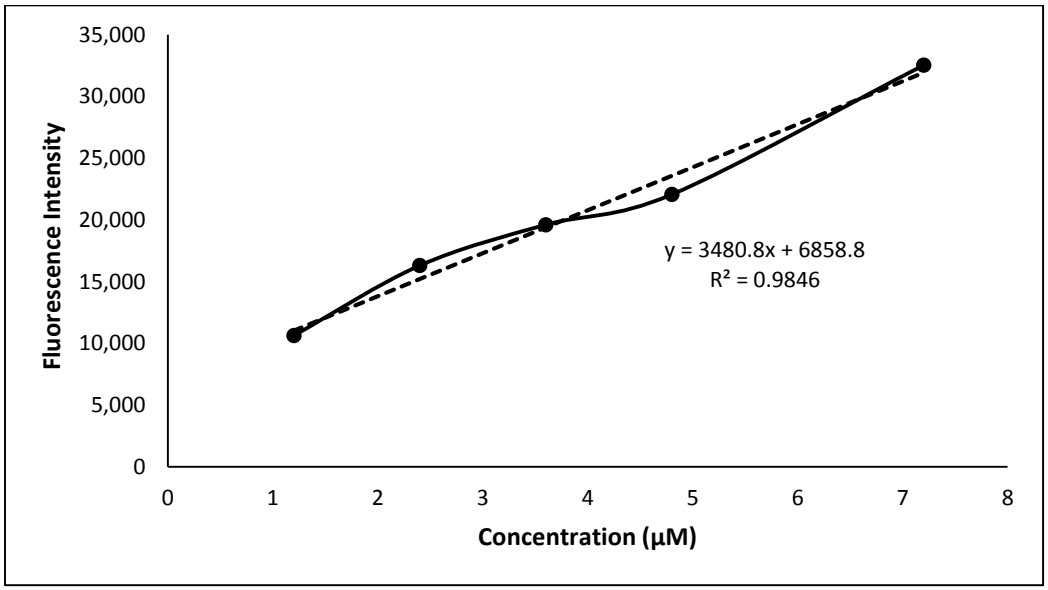

Figure 5.4: Fluorescence peak emissions (643 nm) of Nile red.

Figure 5.5 shows the fluorescence intensity at 643 nm of 4 µM Nile red and 12 µM DPH as a function of pressure. Excitation of Nile red was done at 545 nm, so no

effect is expected from DPH. Even though it was expected that the fluorescence would increase due to the increase in concentration of Nile red after volume reduction due to pressurization, fluorescence actually decreased.

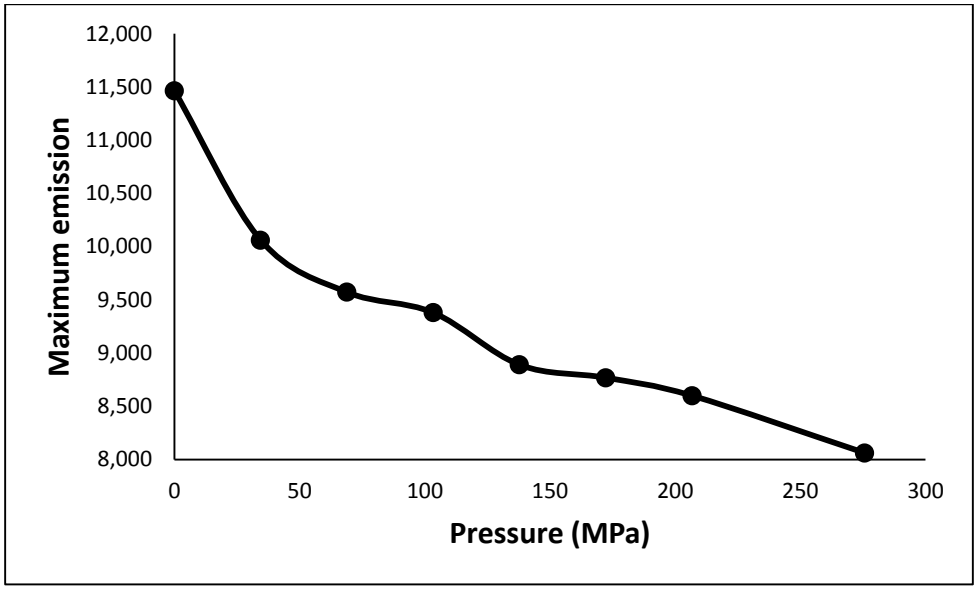

Figure 5.5: Fluorescence intensity at 643 nm during pressurization of 4 µM Nile red and 12 µM DPH, with excitation at 545 nm.

The decrease in fluorescence of Nile red during pressurization is likely due to phase change in the mineral oil, which would expel the Nile red and prevent it from emitting fluorescence. So even if the FRET system between Nile red and DPH would have given a signal from inside the pressure vessel, the dependency of Nile red on the stability of lipids makes it unsuitable as a pressure sensor.

5.3.b. In situ Studies of Microbial Inactivation during HPP

Figure 5.6, Figure 5.8, and Figure 5.10 show the fluorescence intensity at 622 nm during the three different high pressure processes for *Enterobacter aerogenes* suspensions with propidium iodide; while Figure 5.7, Figure 5.9, and Figure 5.11 show each of the relative changes of emission intensity during depressurization, calculated as $1 - [EI_i - EI]/EI$ (so it would be easier to compare with the relative volume change of water, expressed as the change of density from atmospheric pressure to each pressure). In the blank samples, without propidium iodide, no emission was detected at 622 nm. As expected, at higher pressures the emission intensity increased at a higher rate. During pressure hold time, the emission intensity also increased. As mentioned previously, propidium iodide fluorescence emission corresponded to damage of the external membranes and inactivation of bacterial cells (Boulos *et al.*, 1999; Nebe-von Caron *et al.*, 1998). After the second cycle at 267 MPa for 3 min shown in Figure 5.6, in which additional bacterial inactivation was achieved, the third cycle at 345 MPa for 3 min did not cause additional increase in fluorescence intensity; only a small increase between 267 MPa and at 345 MPa was detected, which was attributed to the increase in concentration of propidium iodide due to pressurization. The fluorescence intensities after depressurization in the second and third cycles were the same.

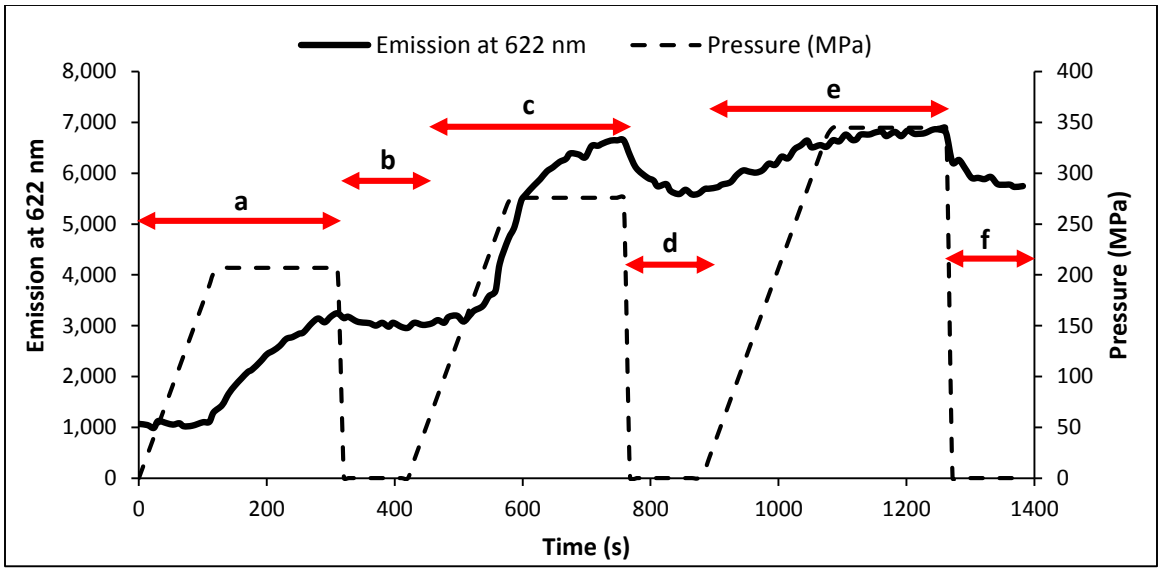

Figure 5.6: Emission intensity at 622 nm during a process consisting of: a)Pressurization to 207 MPa (30 kpsi) and hold time of 3 min; b)instant depressurization and held at atmospheric pressure for 2 min; c)pressurization to 276 MPa (40 kpsi) and hold time of 3 min; d)instant depressurization and held at atmospheric pressure for 2 min; e)pressurization to 345 MPa (50 kpsi) and hold time of 3 min; f)instant depressurization and held at atmospheric pressure for 2 min.

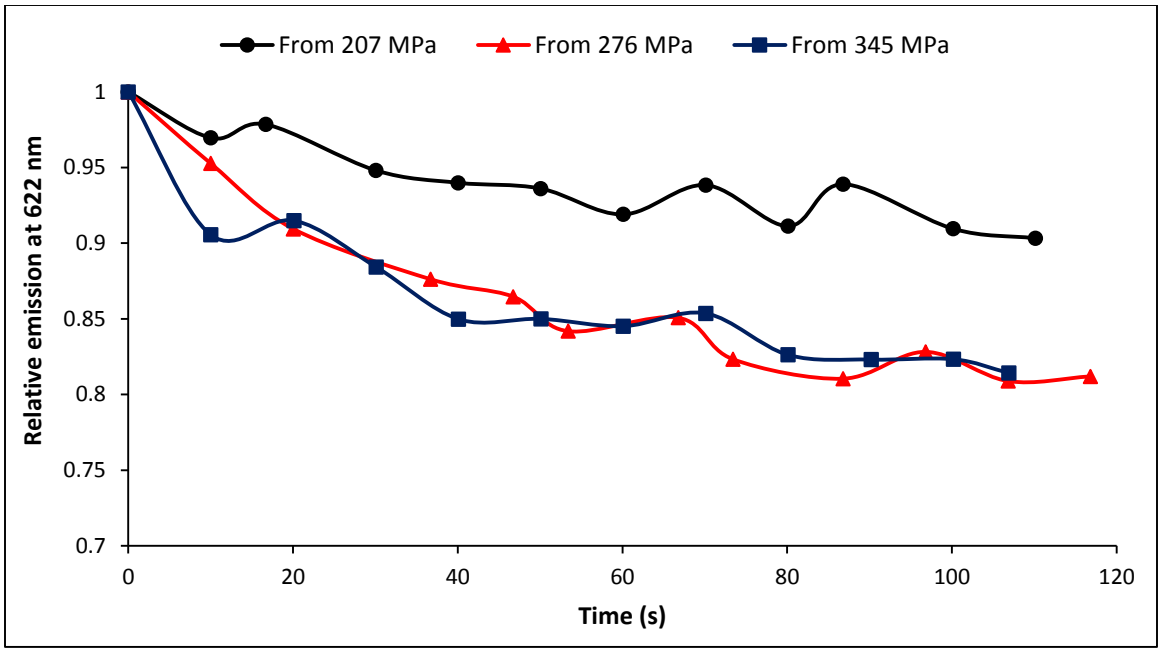

Figure 5.7: Relative change of emission intensity at 622 nm after depressurization of each of the three pressure holding stages on Figure 5.6.

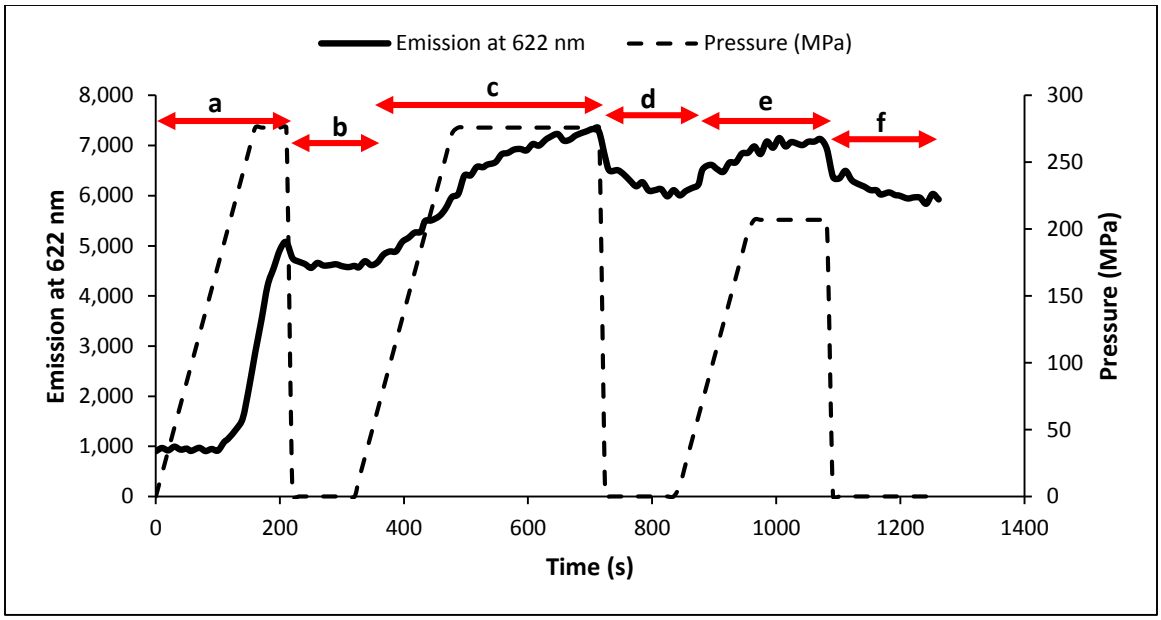

Figure 5.8: Emission intensity at 622 nm during a process consisting of: a)Pressurization to 276 MPa (40 kpsi) and hold time of 45 s; b)instant depressurization and held at atmospheric pressure for 2 min; c)pressurization to 276 MPa (40 kpsi) and hold time of 4 min; d)instant depressurization and held at atmospheric pressure for 2 min; e)pressurization to 207 MPa (30 kpsi) and hold time of 2 min; f)instant depressurization and held at atmospheric pressure for 3 min.

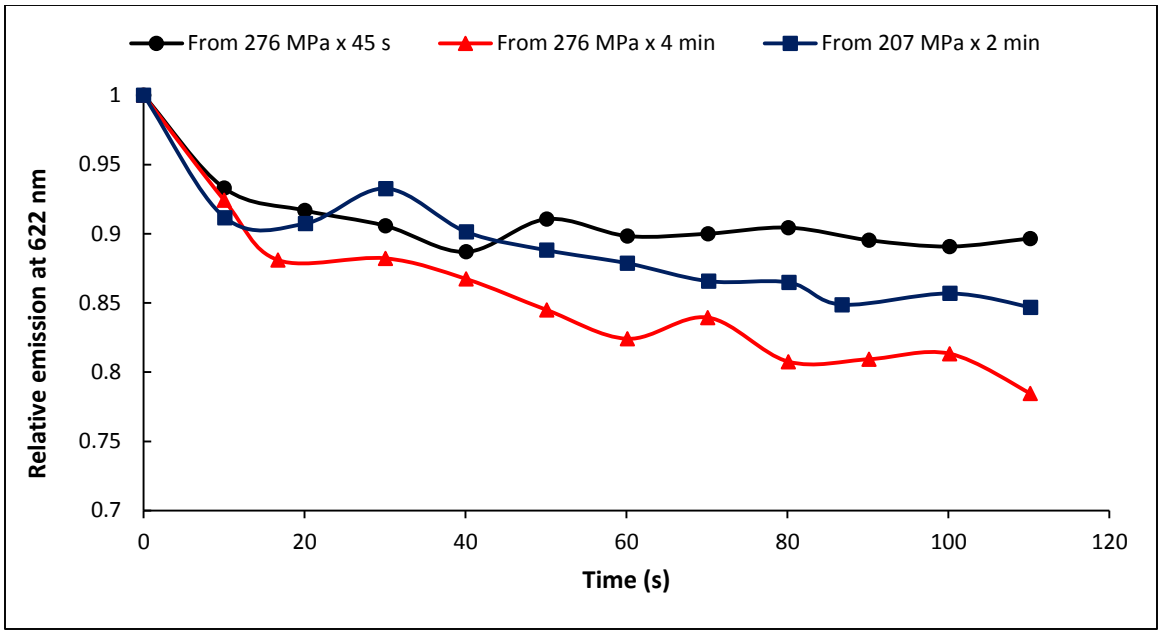

Figure 5.9: Relative change of emission intensity at 622 nm after depressurization of each of the three pressure holding stages on Figure 5.8.

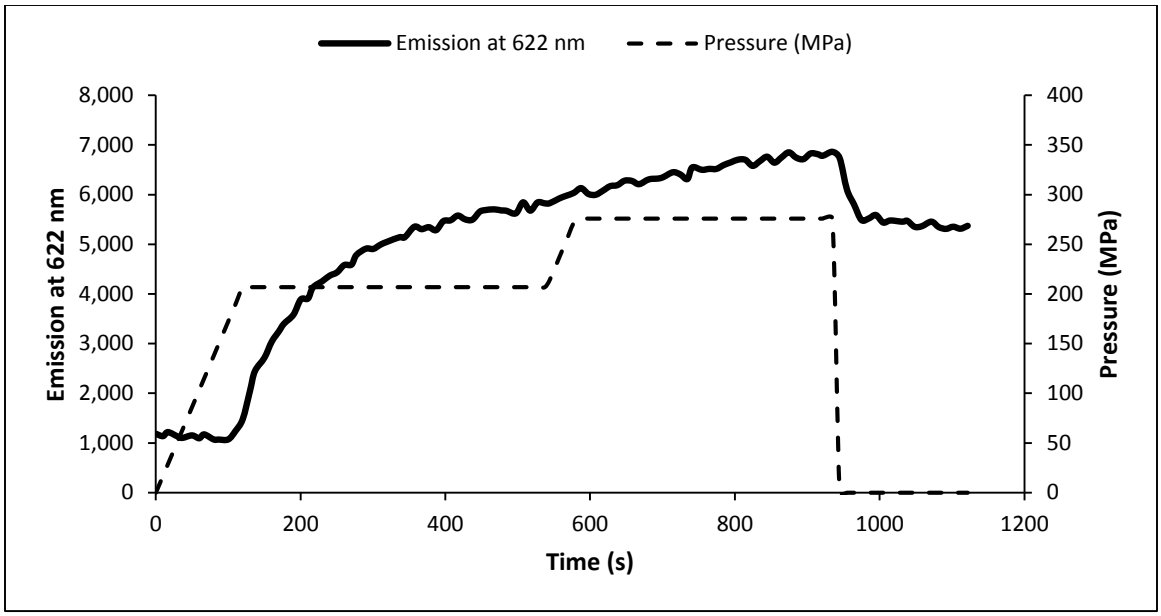

Figure 5.10: Emission intensity at 622 nm during a process consisting of: a)pressurization to 207 MPa (30 kpsi) and hold time of 7 min; b)pressurization to 276 MPa (40 kpsi) and hold time of 6 min; c)instant depressurization and held at atmospheric pressure for 3 min.

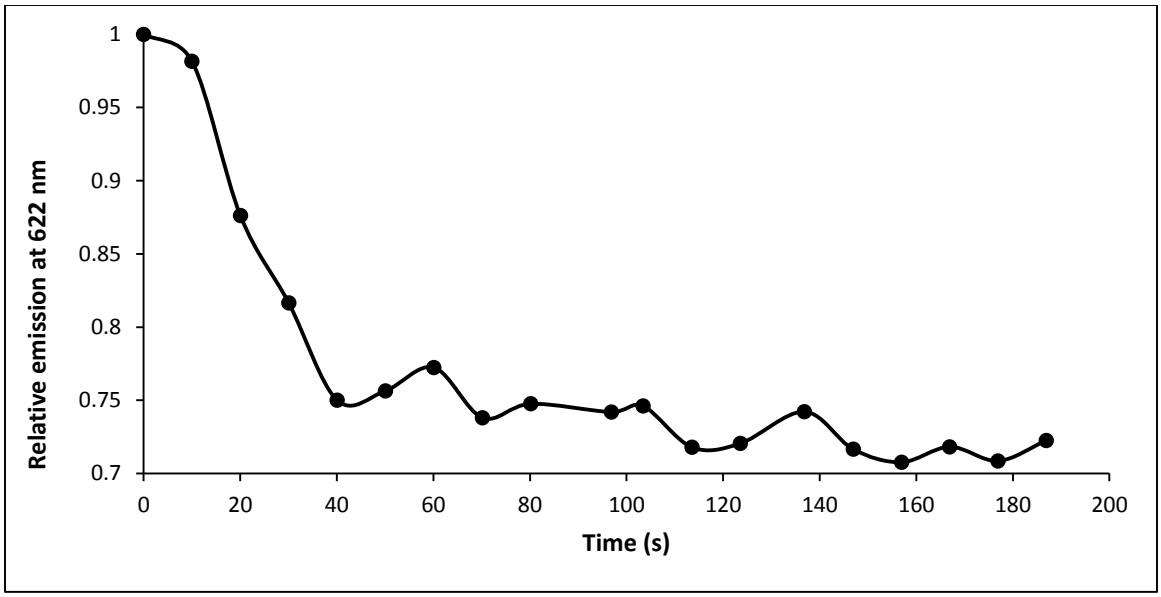

Figure 5.11: Relative change of emission intensity at 622 nm after depressurization of in the process on Figure 5.10.

The emission intensity decreased after depressurization, but it was not instantaneous in any of the cases. Moreover, except for the first decompression cycles corresponding to 207 MPa for 5 min and 276 MPa for 45 s from Figure 5.6 and Figure 5.8, respectively, the decrease in emission intensity was higher than expected, based purely on the decrease in concentration due to volumetric expansion. Since water is the predominant component, it is expected that the compressibility of our system will closely resemble that of water. Table 5-1 shows the volume change of water upon decompression based on the data published by NIST (Harvey *et al.*, 2010).

Table 5-1: Change in volume of water between atmospheric pressure and high pressures.

Pressure (MPa)	Relative change in volume
207	7.5%
276	9.6%
345	11.4%

The processing conditions were chosen to allow for only partial microbial inactivation and in many cases for fluorescence intensities below the plateau value, to allow for detection of further changes during depressurization or subsequent steps. Table 5-2 shows the microbial reduction achieved at each independent stage of the process. In all cases it was negligible, however it is important to mention that microbial reduction was expressed in log scale while the increase of emission would be linearly proportional to the damaged cells.

Table 5-2: Microbial reductions achieved at each stage of the processes.

Process	Reduction (log cfu/mL)
276 MPa x 45 s	0.43 ± 0.008
207 MPa x 7 min	0.14 ± 0.014
207 MPa x 3 min	0.08 ± 0.044

No increase of emission was detected with *Listeria innocua* or *Saccharomyces cerevisiae*, even though the processing conditions had shown in previous experiments (see section 4) to achieve reductions higher than 1 log cfu/mL. We think this was because the Gram + cell wall of *Listeria inoocua* allowed very little dye to migrate. In case of *Saccharomyces cerevisiae*, it has been suggested that inactivation of yeast due to pressure is not related to external membrane rupture (Brul *et al.*, 2000), but it also could be because overall available nucleic acid concentration compared to bacterial suspensions caused lower signals not detectable by our instruments.

The effects of the pressurization and hold time stages have been studied (McClements *et al.*, 2001; Mussa *et al.*, 1998; Basak and Ramaswamy, 1996), as well as the effect of pressurization and depressurization rates (Syed *et al.*, 2013; Chapleau *et al.*, 2006; Rademacher *et al.*, 2002), but so far the effects of the depressurization stage in HPP had not been isolated. By measuring the fluorescence of propidium iodide during HPP we can pinpoint the moment when microbial inactivation took place. As shown in Figure 5.6, Figure 5.8, and Figure 5.10, the emission of propidium iodide increased during pressurization and hold time in all our processes, but not during depressurization. Figure 5.8 shows a process where the first cycle (267 MPa for 45 s) was specifically set up to achieve only partial inactivation; still the first decompression did not increase the fluorescence emission, which only happened in the second cycle. Therefore, no inactivation took place during the depressurization stage.

Moreover, in most of the cycles the fluorescence of propidium iodide actually decreased after depressurization and during the time the microbial suspensions were held at atmospheric pressure in between cycles or at the end of the processes, as seen in Figures Figure 5.7, Figure 5.9, and Figure 5.11. If this decrease in fluorescence would have originated only from the decrease in propidium iodide concentration due to volumetric expansion during decompression, the change in relative fluorescence emission in the figures would have been similar to the change in volume of water at the given pressures in Table 5-1, but they were actually higher than that. For example, after the second cycle at 276 MPa in Figure 5.7, the average loss of emission after the value stabilized was 18.4% while the change in water volume was only 9.6%. In Figure 5.11 the change is more dramatic, after 7 min at 207 MPa and 6 min at 267 MPa the average loss of emission was 27.3% while the change in water volume after decompression still was 9.6%.

As mentioned previously, propidium iodide fluorescence originates from binding with nucleic acids. Therefore, the unusual reduction in fluorescence after depressurization would have to be caused by propidium iodide separating from DNA or RNA at atmospheric pressure. Mentré and Hoa (2001) pointed out that high pressure has a stabilizing effect on DNA hydrogen bonds. Krzyżaniak *et al.* (1994) studied the conformation changes of RNA at 600 MPa and 800 MPa and determined that it could be getting aggregated or condensed. Therefore it is unlikely that pressure would favor DNA/RNA - propidium iodide binding so that after depressurization they separate and give a lower fluorescence.

We think that the cause of the unexpected change in fluorescence is ribosome disassociation. Infante *et al.* (1982) studied the thermodynamics of reversible *E. coli* ribosome disassociation between 20 MPa and 120 MPa. Gross *et al.* (1993) observed disassociation starting at 60 MPa in ribosomal preparations. Lu *et al.* (1997) observed loss on rat ribosome activity immediately after HPP, but it was recovered after an incubation period. Niven *et al.* (1999) detected conformation changes in *E. coli* ribosomes between 50 MPa and 250 MPa, and suggested that cell death during HPP was related to protein synthesis inhibition. If the ribosomes of *Enterobacter aerogenes* were also reversibly disassociating at high pressure, that would open additional sites for their RNA to interact with propidium iodide and increase the fluorescence signal. Upon depressurization, when the ribosome subunits associating back, the some of the bound propidium iodide would be expelled and the fluorescence would decrease beyond the expected value due to volume expansion. This would also explain why it happened over a period of time and not instantaneously.

One additional observation that comes from our data is that ribosome disassociation would take place after membrane rupture. That would explain why after processes at higher pressure and longer times, such 207 MPa for 7 min and 276 MPa for 6 min shown in Figure 5.11, the difference between the fluorescence decrease after decompression and the water volume change higher (27.3% vs. 9.6%) compared to a shorter process like 276 MPa for 45 s in Figure 5.9 where the difference was much smaller (10% vs. 9.6%). Additionally, pressure cycling would be affecting ribosome disassociation, which would explain why the fluorescence decrease after the third cycle

in Figure 5.9 (207 MPa for 2 min) was 16.6% and the decrease after the first cycle in Figure 5.7 (207 MPa for 3 min) was 7.6%. The volume change of water at 207 MPa is 7.5% (Table 5-1). This could develop into an interesting area of research, looking at the effect of the wait time between pressure cycles.

Another possible interpretation of the decrease in fluorescence would be that some cells were able to pump propidium iodide out after decompression. Pagán and Mackey (2000) observed propidium iodide uptake by *E. coli* cells in stationary phase during HPP but not when exposed to the dye after processing, suggesting that the cells were able to reseal their membrane. However, this also indicates that the dye wasn't actively pumped out by the cells, some of which were viable and some not.

6. Conclusions

The data supports the hypothesis that, when subjected to external hydrostatic pressure during high pressure processing, pressure and shear stress gradients form inside heterogeneous solid foods that would affect microbial inactivation. However, the gradients were not as extensive as originally thought. They were restricted to the close vicinities of the hard inclusions, very likely only a few micrometers away from the interface between the soft material and the hard inclusion. These findings would be important for the high pressure processing of heterogeneous solid foods where the amount of inclusions could vary, as the process should be designed for the worst possible scenario in which the volume of hard inclusions offer the maximum protection to the microorganisms.

The differences in the changes of inactivation of *Listeria innocua* and *Saccharomyces cerevisiae* suggest that these organisms respond differently to pressure and shear stress. While the inactivation of *Listeria* decreased monotonically when the volume fraction of hard inclusions increased, the inactivation of *Saccharomyces* first decreased and then increased when a higher volume fraction was incorporated. This suggests that pressure and shear have an antagonistic effect in the inactivation of *Saccharomyces*, possibly because shear would reduce the development of buckling and alleviate stress in the globular yeast cell wall.

The FRET system composed of Nile red and DPH was shown to be unsuitable as a pressure sensor. Besides the inability of our equipment to detect any emission from Nile

red after exciting DPH at 390 nm, the fluorescence of Nile red was also shown to be affected by the pressure, likely because of phase change in the lipids which would expel Nile red and reduce the fluorescence.

Cell wall and membrane rupture was detected in *Enterobacter aerogenes* during pressurization and hold time, but not during depressurization. Moreover, a higher than expected decrease in fluorescence after depressurization indicates that ribosomes would be disassociating at high pressure and associating back 20 s to 60 s after depressurization, from pressures between 207 MPa and 345 MPa. It is also likely that the ribosomes disassociation took place after membrane rupture.

7. Future Work

Numerical simulations of the stress distribution in the model systems with plaster of Paris inclusions during high pressure processing are needed to confirm if adding more inclusions would change the distribution of stress non-uniform regions from medium shear – medium pressure to high shear – low pressure. This could support the explanation made in this project on why the change in *Listeria innocua* and *Saccharomyces cerevisiae* reduction is different between the model system of agar gel with different volumes of plaster particles.

The development of a procedure to apply pure static shear on a material would allow to study the independent effects of pressure and shear on microbial inactivation and expand the findings in this project, which only studied the effects of pressure stress alone and the combination of pressure and shear stress.

The measurement of Poisson's ratio at high pressure would provide valuable data to develop a model to more accurately describe the stress distribution in materials with hard inclusions during high pressure processing. This project has shown that shear stress would develop and pressure would decrease around the inclusions, but the gradients or the extension of the non-uniformity regions were not quantified due to the unavailability of a second mechanical property of the material.

Further studies are required to confirm if ribosome disassociation is responsible for the decrease in fluorescence after the pressure had been released. It would be

necessary to extract the ribosomes and suspend them without damaging their structure, and measure their fluorescence with propidium iodide during high pressure processing. Additionally, modifications in the equipment could be made to increase the sensitivity of the method and measure fluorescence of more resistant organisms, such as Gram positive bacteria. Finally, a study of the effect of the wait time between cycles in pressure cycling could be made and relate to the observed decrease in fluorescence several seconds after pressure release.

8. Acknowledgments of Previous Publications

The Introduction section of this thesis is partially taken from our previously published book chapter: Karwe, M. V., Maldonado, J. and Mahadevan, S. 2014. *High Pressure Processing: Current Status*, in Conventional and Advanced Food Processing Technologies (ed S. Bhattacharya), John Wiley & Sons, Ltd, Chichester, UK. doi: 10.1002/9781118406281.ch24.

The Theoretical Background (section 2.2) of this thesis is partially taken from our manuscript submitted for publication: Nair, A., Maldonado, J. A., Miyazawa, Y., Cuitiño, A., Schaffner, D. W., Karwe, M. V. *Numerical Simulation of Stress Distribution in Heterogeneous Solids during High Pressure Processing*. Journal of Food Engineering, submitted on November 12.

9. Bibliography

1. Abdul Ghani A.G., Farid M.M. 2007. Numerical Simulation of Solid–Liquid Food Mixture in a High Pressure Processing Unit Using Computational Fluid Dynamics. Journal of Food Engineering 80(4):1031-42.
2. Abid M., Jabbar S., Hu B., Hashim M.M., Wu T., Wu Z., Khan M.A., Zeng X. 2014. Synergistic Impact of Sonication and High Hydrostatic Pressure on Microbial and Enzymatic Inactivation of Apple Juice. LWT - Food Science and Technology 59(1):70-6.
3. Ananta E., Heinz V., Schlüter O., Knorr D. 2001. Kinetic Studies on High-Pressure Inactivation of Bacillus Stearothermophilus Spores Suspended in Food Matrices. Innovative Food Science & Emerging Technologies 2(4):261-72.
4. Ananta E., Knorr D. 2009. Comparison of Inactivation Pathways of Thermal or High Pressure Inactivated Lactobacillus Rhamnosus Atcc 53103 by Flow Cytometry Analysis. Food Microbiology 26(5):542-6.
5. Balasubramaniam V.M.B. 2009. Opportunities and Challenges in Pressure-Assisted Thermal Sterilization of Low-Acid Foods. International Forum on Emerging Technologies in Food Processing. University of Illinois (Urbana-Champaign), USA.
6. Barbosa-Cánovas G.V., Tapia M.a.S., Cano M.P. 2005. Novel Food Processing Technologies. Boca Raton: CRC Press.
7. Basak S., Ramaswamy H.S. 1996. Ultra High Pressure Treatment of Orange Juice: A Kinetic Study on Inactivation of Pectin Methyl Esterase. Food Research International 29(7):601-7.
8. Bayındırlı A., Alpas H., Bozoğlu F., Hızal M. 2006. Efficiency of High Pressure Treatment on Inactivation of Pathogenic Microorganisms and Enzymes in Apple, Orange, Apricot and Sour Cherry Juices. Food Control 17(1):52-8.
9. Benito A., Ventoura G., Casadei M., Robinson T., Mackey B. 1999. Variation in Resistance of Natural Isolates Ofescherichia Coli O157 to High Hydrostatic Pressure, Mild Heat, and Other Stresses. Applied and environmental microbiology 65(4):1564-9.
10. Black E.P., Huppertz T., Fitzgerald G.F., Kelly A.L. 2007. Baroprotection of Vegetative Bacteria by Milk Constituents: A Study of Listeria Innocua. Int. Dairy J. 17(2):104-10.
11. Boudjema M., Santos I.B., McCall K.R., Guyer R.A., Boitnott G.N. 2003. Linear and Nonlinear Modulus Surfaces in Stress Space, from Stress-Strain Measurements on Berea Sandstone. Nonlin. Processes Geophys. 10(6):589-97.
12. Boulos L., Prévost M., Barbeau B., Coallier J., Desjardins R. 1999. Live/Dead® Baclight™: Application of a New Rapid Staining Method for Direct Enumeration of Viable and Total Bacteria in Drinking Water. Journal of Microbiological Methods 37(1):77-86.
13. Bower A.F. 2010. Applied Mechanics of Solids. Boca Raton: CRC Press.

14. Bradley D.W., Hess R.A., Tao F., Sciaba-Lentz L., Remaley A.T., Laugharn J.A., Jr., Manak M. 2000. Pressure Cycling Technology: A Novel Approach to Virus Inactivation in Plasma. Transfusion 40(2):193-200.
15. Brennan J.G. 2006. Food Processing Handbook. Weinheim: Wiley-VCH.
16. Brul S., Rommens A.J.M., Verrips C.T. 2000. Mechanistic Studies on the Inactivation of Saccharomyces Cerevisiae by High Pressure. Innovative Food Science & Emerging Technologies 1(2):99-108.
17. Bulut S., Waites W.M., Mitchell J.R. 1999. Effects of Combined Shear and Thermal Forces on Destruction of Microbacterium Lacticum. Applied and environmental microbiology 65(10):4464-9.
18. Butz P., Edenharder R., Fister H., Tauscher B. 1997. The Influence of High Pressure Processing on Antimutagenic Activities of Fruit and Vegetable Juices. Food Research International 30(3–4):287-91.
19. Buzrul S., Alpas H., Largeteau A., Bozoglu F., Demazeau G. 2008a. Compression Heating of Selected Pressure Transmitting Fluids and Liquid Foods During High Hydrostatic Pressure Treatment. Journal of Food Engineering 85(3):466-72.
20. Buzrul S., Alpas H., Largeteau A., Demazeau G. 2008b. Inactivation of Escherichia Coli and Listeria Innocua in Kiwifruit and Pineapple Juices by High Hydrostatic Pressure. International Journal of Food Microbiology 124(3):275-8.
21. Chapleau N., Ritz M., Delépine S., Jugiau F., Federighi M., de Lamballerie M. 2006. Influence of Kinetic Parameters of High Pressure Processing on Bacterial Inactivation in a Buffer System. International Journal of Food Microbiology 106(3):324-30.
22. Cheftel J.C. 1995. Review : High-Pressure, Microbial Inactivation and Food Preservation / Revisión: Alta-Presión, Inactivación Microbiológica Y Conservación De Alimentos. Food Science and Technology International 1(2-3):75-90.
23. Chung Y.K., Vurma M., Turek E.J., Chism G.W., Yousef A.E. 2005. Inactivation of Barotolerant Listeria Monocytogenes in Sausage by Combination of High-Pressure Processing and Food-Grade Additives. J Food Prot 68(4):744-50.
24. Clegg R.M. 1995. Fluorescence Resonance Energy Transfer. Current Opinion in Biotechnology 6(1):103-10.
25. D'Souza T., Karwe M., Schaffner D.W. 2012. Effect of High Hydrostatic Pressure and Pressure Cycling on a Pathogenic Salmonella Enterica Serovar Cocktail Inoculated into Creamy Peanut Butter. Journal of Food Protection® 75(1):169-73.
26. De Ancos B., Gonzalez E., Cano M.P. 2000. Effect of High-Pressure Treatment on the Carotenoid Composition and the Radical Scavenging Activity of Persimmon Fruit Purees. Journal of Agricultural and Food Chemistry 48(8):3542-8.
27. Denys S., Ludikhuyze L.R., Van Loey A.M., Hendrickx M.E. 2000a. Modeling Conductive Heat Transfer and Process Uniformity During Batch High-Pressure Processing of Foods. Biotechnology Progress 16(1):92-101.
28. Denys S., Van Loey A.M., Hendrickx M.E. 2000b. A Modeling Approach for Evaluating Process Uniformity During Batch High Hydrostatic Pressure Processing: Combination of a Numerical Heat Transfer Model and Enzyme Inactivation Kinetics. Innovative Food Science & Emerging Technologies 1(1):5-19.

29. Doblado R., Frías J., Vidal-Valverde C. 2007. Changes in Vitamin C Content and Antioxidant Capacity of Raw and Germinated Cowpea (Vigna Sinensis Var. Carilla) Seeds Induced by High Pressure Treatment. Food Chemistry 101(3):918-23.
30. Dogan C., Erkmen O. 2004. High Pressure Inactivation Kinetics of Listeria Monocytogenes Inactivation in Broth, Milk, and Peach and Orange Juices. Journal of Food Engineering 62(1):47-52.
31. Doona C.J., Feeherry F.E. 2007. High Pressure Processing of Foods, 1st ed. Ames, Iowa, Chicago: Blackwell Pub., IFT Press.
32. Dornenburg H., Knorr D. 1993. Cellular Permeabilization of Cultured Plant-Tissues by High Electric-Field Pulses or Ultra High-Pressure for the Recovery If Secondary Metabolites. Food Biotechnol. 7(1):35-48.
33. Earnshaw R.G. 1995. High Pressure Microbial Inactivation Kinetics. In: Ledward D.A., Johnston D.E., Earnshaw R.G., Hasting A.P.M., editors. High Pressure Processing of Foods. Loughborough: Nottingham University Press. p. viii, 208 p.
34. Farid M.M., inventor; Auckland Uniservices Limited, assignee. 2006. Pressure Assisted Thermal Sterilisation or Pasteurisation Method and Apparatus. USA patent.
35. Fernández García A., Butz P., Bognàr A., Tauscher B. 2001. Antioxidative Capacity, Nutrient Content and Sensory Quality of Orange Juice and an Orange-Lemon-Carrot Juice Product after High Pressure Treatment and Storage in Different Packaging. Eur Food Res Technol 213(4-5):290-6.
36. Förster T. 1948. Zwischenmolekulare Energiewanderung Und Fluoreszenz. Annalen der Physik 437(1-2):55-75.
37. Friedrich O., Kress K.R., Hartmann M., Frey B., Sommer K., Ludwig H., Fink R.H.A. 2006. Prolonged High-Pressure Treatments in Mammalian Skeletal Muscle Result in Loss of Functional Sodium Channels and Altered Calcium Channel Kinetics. Cell Biochem Biophys 45(1):71-83.
38. Gercek H. 2007. Poisson's Ratio Values for Rocks. International Journal of Rock Mechanics and Mining Sciences 44(1):1-13.
39. Gould G.W. 1995. The Microbe as a High Pressure Target. In: Ledward D.A., Johnston D.E., Earnshaw R.G., Hasting A.P.M., editors. High Pressure Processing of Foods. Loughborough: Nottingham University Press. p. viii, 208 p.
40. Gross M., Lehle K., Jaenicke R., Nierhaus K.H. 1993. Pressure-Induced Dissociation of Ribosomes and Elongation Cycle Intermediates. European Journal of Biochemistry 218(2):463-8.
41. Ha T. 2001. Single-Molecule Fluorescence Resonance Energy Transfer. Methods 25(1):78-86.
42. Hartmann C. 2002. Numerical Simulation of Thermodynamic and Fluid-Dynamic Processes During the High-Pressure Treatment of Fluid Food Systems. Innovative Food Science and Emerging Technologies 3(1):11-8.
43. Hartmann C., Delgado A. 2002. Numerical Simulation of Convective and Diffusive Transport Effects on a High-Pressure-Induced Inactivation Process. Biotechnology and bioengineering 79(1):94-104.

44. Hartmann C., Delgado A. 2003. The Influence of Transport Phenomena During High-Pressure Processing of Packed Food on the Uniformity of Enzyme Inactivation. Biotechnology and bioengineering 82(6):725-35.
45. Hartmann C., Delgado A. 2004. Numerical Simulation of the Mechanics of a Yeast Cell under High Hydrostatic Pressure. Journal of biomechanics 37(7):977-87.
46. Hartmann C., Delgado A., Szymczyk J. 2003. Convective and Diffusive Transport Effects in a High Pressure Induced Inactivation Process of Packed Food. Journal of Food Engineering 59(1):33-44.
47. Harvey A.H., Peskin A.P., Klein S.A. 2010. Nist/Asme Steam Properties Database. 2.2 ed: National Institute of Standards and Technology.
48. Hayman M.M., Anantheswaran R.C., Knabel S.J. 2007. The Effects of Growth Temperature and Growth Phase on the Inactivation of Listeria Monocytogenes in Whole Milk Subject to High Pressure Processing. Int J Food Microbiol 115(2):220-6.
49. Hayman M.M., Anantheswaran R.C., Knabel S.J. 2008a. Heat Shock Induces Barotolerance in Listeria Monocytogenes. J Food Prot 71(2):426-30.
50. Hayman M.M., Kouassi G.K., Anantheswaran R.C., Floros J.D., Knabel S.J. 2008b. Effect of Water Activity on Inactivation of Listeria Monocytogenes and Lactate Dehydrogenase During High Pressure Processing. Int J Food Microbiol 124(1):21-6.
51. He X., Kim S.S., Park S.J., Seong D.H., Yoon W.B., Lee H.Y., Park D.S., Ahn J. 2010. Combined Effects of Probiotic Fermentation and High-Pressure Extraction on the Antioxidant, Antimicrobial, and Antimutagenic Activities of Deodeok (Codonopsis Lanceolata). J Agric Food Chem 58(3):1719-25.
52. Hendrickx M.E.G., Knorr D.W. 2002. Ultra High Pressure Treatments of Foods. New York: Kluwer Academic/Plenum Publishers.
53. Heremans K. 1995. High Pressure Effects on Biomolecules. In: Ledward D.A., Johnston D.E., Earnshaw R.G., Hasting A.P.M., editors. High Pressure Processing of Foods. Loughborough: Nottingham University Press. p. viii, 208 p.
54. Huang K.C., Mukhopadhyay R., Wen B., Gitai Z., Wingreen N.S. 2008. Cell Shape and Cell-Wall Organization in Gram-Negative Bacteria. Proceedings of the National Academy of Sciences 105(49):19282-7.
55. Infante A.A., Demple B., Chaires J.B. 1982. Analysis of the Escherichia Coli Ribosome-Ribosomal Subunit Equilibrium Using Pressure-Induced Dissociation. The Journal of biological chemistry 257(1):80-7.
56. invitrogen. 2006. Propidium Iodide Nucleic Acid Stain. In: invitrogen, editor. Molecular Probes.
57. Isaacs N.S., Chilton P. 1995. Studies on the Inactivation by High Pressure of Micro-Organisms. In: Ledward D.A., Johnston D.E., Earnshaw R.G., Hasting A.P.M., editors. High Pressure Processing of Foods. Loughborough: Nottingham University Press. p. viii, 208 p.
58. Jain B., Das K. 2006. Fluorescence Resonance Energy Transfer between Dph and Nile Red in a Lipid Bilayer. Chemical Physics Letters 433(1–3):170-4.
59. Kaletunç G., Lee J., Alpas H., Bozoglu F. 2004. Evaluation of Structural Changes Induced by High Hydrostatic Pressure in Leuconostoc Mesenteroides. Applied and environmental microbiology 70(2):1116-22.

60. Khurana M. 2012. Temperature Distribution in Vertical and Horizontal High Pressure Vessels and Its Impact on Food Safety. Rutgers University. Graduate School--New Brunswick.,. p. xxiii, 201 p.
61. Khurana M., Karwe M.V. 2009. Numerical Prediction of Temperature Distribution and Measurement of Temperature in a High Hydrostatic Pressure Food Processor. Food Bioprocess Technol 2(3):279-90.
62. Klärner F.-G., Diedrich M.K., Dierkes G., Gehrke J.-S. 1998. Organic Reactions at High Pressure. The Effect of Pressure on Cyclizations and Homolytic Bond Cleavage. In: Isaacs N.S., editor. High Pressure Food Science, Bioscience and Chemistry. Cambridge, UK: The Royal Society of Chemistry. p. 3-11.
63. Knoerzer K., Buckow R., Chapman B., Juliano P., Versteeg C. 2010a. Carrier Optimisation in a Pilot-Scale High Pressure Sterilisation Plant – an Iterative Cfd Approach Employing an Integrated Temperature Distributor (Itd). Journal of Food Engineering 97(2):199-207.
64. Knoerzer K., Buckow R., Versteeg C. 2010b. Adiabatic Compression Heating Coefficients for High-Pressure Processing – a Study of Some Insulating Polymer Materials. Journal of Food Engineering 98(1):110-9.
65. Knoerzer K., Juliano P., Gladman S., Versteeg C., Fryer P.J. 2007. A Computational Model for Temperature and Sterility Distributions in a Pilot-Scale High-Pressure High-Temperature Process. AIChE Journal 53(11):2996-3010.
66. Koseki S., Yamamoto K. 2007. A Novel Approach to Predicting Microbial Inactivation Kinetics During High Pressure Processing. International Journal of Food Microbiology 116(2):275-82.
67. Krzyżaniak A., Barciszewski J., Fürste J.P., Bald R., Erdmann V.A., Salański P., Jurczak J. 1994. A-Z-Rna Conformational Changes Effected by High Pressure. International Journal of Biological Macromolecules 16(3):159-62.
68. Lee H.Y., He X., Ahn J. 2010. Enhancement of Antimicrobial and Antimutagenic Activities of Korean Barberry (Berberis Koreana Palib.) by the Combined Process of High-Pressure Extraction with Probiotic Fermentation. Journal of the science of food and agriculture 90(14):2399-404.
69. Lu B., Li Q., Liu W.-Y., Ruan K.-c. 1997. Effects of Hydrostatic Pressure on the Activity of Rat Ribosome and Cell-Free Translation System. IUBMB Life 43(3):499-506.
70. Ludwig H., Bieler C., Hallbauer K., Wilhelm S. 1992. Inactivation of Microorganisms by Hydrostatic Pressure. In: C. Balny R.H., K. Heremans, P. Masson, editor. High Pressure and Biotechnology: Colloque INSERM/John Libbey Eurotext Ltd. p. 25-32.
71. Ly-Nguyen B., Van Loey A.M., Smout C., ErenÖzcan S., Fachin D., Verlent I., Truong S.V., Duvetter T., Hendrickx M.E. 2003. Mild-Heat and High-Pressure Inactivation of Carrot Pectin Methylesterase: A Kinetic Study. Journal of Food Science 68(4):1377-83.
72. Madigan M.T., Martinko J.M., Brock T.D. 2006. Brock Biology of Microorganisms, 11th ed. Upper Saddle River, NJ: Pearson Prentice Hall.
73. Mahadevan S., Karwe M.V. 2011. Enhanced Infusion under High Pressure: New Insights. International Congress on Engineering and Food. Athens, Greece.

74. Maitland J.E., Boyer R.R., Eifert J.D., Williams R.C. 2011. High Hydrostatic Pressure Processing Reduces Salmonella Enterica Serovars in Diced and Whole Tomatoes. International Journal of Food Microbiology 149(2):113-7.
75. Manas P., Mackey B.M. 2004. Morphological and Physiological Changes Induced by High Hydrostatic Pressure in Exponential- and Stationary-Phase Cells of Escherichia Coli: Relationship with Cell Death. Applied and environmental microbiology 70(3):1545-54.
76. McClements J.M., Patterson M.F., Linton M. 2001. The Effect of Growth Stage and Growth Temperature on High Hydrostatic Pressure Inactivation of Some Psychrotrophic Bacteria in Milk. J Food Prot 64(4):514-22.
77. Mentré P., Hoa G.H.B. 2001. Effects of High Hydrostatic Pressures on Living Cells: A Consequence of the Properties of Macromolecules and Macromolecule-Associated Water. International Review of Cytology: Academic Press. p. 1-84.
78. Michiels C., Bartlett D.H., Aertsen A. 2008. High-Pressure Microbiology. Washington, DC: ASM Press.
79. Minerich P.L., Labuza T.P. 2003. Development of a Pressure Indicator for High Hydrostatic Pressure Processing of Foods. Innovative Food Science & Emerging Technologies 4(3):235-43.
80. Moeller R., Horneck G., Rabbow E., Reitz G., Meyer C., Hornemann U., Stöffler D. 2008. Role of DNA Protection and Repair in Resistance of Bacillus Subtilis Spores to Ultrahigh Shock Pressures Simulating Hypervelocity Impacts. Applied and environmental microbiology 74(21):6682-9.
81. Mussa D.M., Ramaswamy H.S., Smith J.P. 1998. High Pressure (Hp) Destruction Kinetics of Listeria Monocytogenes Scott a in Raw Milk. Food Research International 31(5):343-50.
82. Narwankar S.P., Flimlin G.E., Schaffner D.W., Tepper B.J., Karwe M.V. 2011. Microbial Safety and Consumer Acceptability of High-Pressure Processed Hard Clams (Mercenaria Mercenaria). Journal of Food Science 76(6):M375-M80.
83. Nebe-von Caron G., Stephens P., Badley R.A. 1998. Assessment of Bacterial Viability Status by Flow Cytometry and Single Cell Sorting. Journal of applied microbiology 84(6):988-98.
84. Nguyen Thi Minh H., Durand A., Loison P., Perrier-Cornet J.M., Gervais P. 2011. Effect of Sporulation Conditions on the Resistance of Bacillus Subtilis Spores to Heat and High Pressure. Applied microbiology and biotechnology 90(4):1409-17.
85. Nicholson W.L., Munakata N., Horneck G., Melosh H.J., Setlow P. 2000. Resistance of Bacillus Endospores to Extreme Terrestrial and Extraterrestrial Environments. Microbiology and Molecular Biology Reviews 64(3):548-72.
86. Nikiyan H., Vasilchenko A., Deryabin D. 2010. Humidity-Dependent Bacterial Cells Functional Morphometry Investigations Using Atomic Force Microscope. International Journal of Microbiology 2010.
87. Niven G.W., Miles C.A., Mackey B.M. 1999. The Effects of Hydrostatic Pressure on Ribosome Conformation in Escherichia Coli: And in Vivo Study Using Differential Scanning Calorimetry. Microbiology (Reading, England) 145 (Pt 2):419-25.

88. Oey I., Lille M., Van Loey A., Hendrickx M. 2008a. Effect of High-Pressure Processing on Colour, Texture and Flavour of Fruit- and Vegetable-Based Food Products: A Review. Trends in Food Science & Technology 19(6):320-8.
89. Oey I., Van der Plancken I., Van Loey A., Hendrickx M. 2008b. Does High Pressure Processing Influence Nutritional Aspects of Plant Based Food Systems? Trends in Food Science & Technology 19(6):300-8.
90. Oliveira A.C., Gaspar L.P., Da Poian A.T., Silva J.L. 1994. Arc Repressor Will Not Denature under Pressure in the Absence of Water. Journal of molecular biology 240(3):184-7.
91. Olivier S.A., Bull M.K., Chapman B. 2012. Bacillus Spp. Spores Produced at Lower Temperatures Are More Resistant to High Pressure Thermal Processes but Mineralization Does Not Predict Relative Resistance. Innovative Food Science & Emerging Technologies 16(0):96-101.
92. Omer M.K., Alvseike O., Holck A., Axelsson L., Prieto M., Skjerve E., Heir E. 2010. Application of High Pressure Processing to Reduce Verotoxigenic E. Coli in Two Types of Dry-Fermented Sausage. Meat Science 86(4):1005-9.
93. Pagán R., Mackey B. 2000. Relationship between Membrane Damage and Cell Death in Pressure-Treated Escherichia Coli Cells: Differences between Exponential- and Stationary-Phase Cells and Variation among Strains. Applied and environmental microbiology 66(7):2829-34.
94. Pavuluri S.R., Kaur B.P. 2014. High Pressure Inactivation Kinetics of Escherichia Coli in Black Tiger Shrimp (Penaeus Monodon). International Conference on Biological, Civil and Environmental Engineering (BCEE-2014). Dubai, UAE. p. 167-9.
95. Pehl M., Werner F., Delgado A. 2002. Experimental Investigation on Thermofluiddynamical Processes in Pressurized Substances. In: Rikimaru H., editor. Progress in Biotechnology: Elsevier. p. 429-35.
96. Perrier-Cornet J.M., Hayert M., Gervais P. 1999. Yeast Cell Mortality Related to a High-Pressure Shift: Occurrence of Cell Membrane Permeabilization. Journal of applied microbiology 87(1):1-7.
97. Perrier-Cornet J.M., Marechal P.A., Gervais P. 1995. A New Design Intended to Relate High Pressure Treatment to Yeast Cell Mass Transfer. Journal of biotechnology 41(1):49-58.
98. Peterson B.W., Sharma P.K., van der Mei H.C., Busscher H.J. 2012. Bacterial Cell Surface Damage Due to Centrifugal Compaction. Applied and environmental microbiology 78(1):120-5.
99. Pope D.H., Smith W.P., Swartz R.W., Landau J.V. 1975. Role of Bacterial Ribosomes in Barotolerance. Journal of bacteriology 121(2):664-9.
100. Popov E.P., Nagarajan S., Lu Z.A. 1976. Mechanics of Materials, 2d ed. Englewood Cliffs, N.J.: Prentice-Hall.
101. Rademacher B., Werner F., Pehl M. 2002. Effect of the Pressurizing Ramp on the Inactivation of Listeria Innocua Considering Thermofluiddynamical Processes. Innovative Food Science & Emerging Technologies 3(1):19-24.

102. Rasanayagam V., Balasubramaniam V.M., Ting E., Sizer C.E., Bush C., Anderson C. 2003. Compression Heating of Selected Fatty Food Materials During High-Pressure Processing. Journal of Food Science 68(1):254-9.
103. Rastogi N.K., Angersbach A., Knorr D. 2000. Synergistic Effect of High Hydrostatic Pressure Pretreatment and Osmotic Stress on Mass Transfer During Osmotic Dehydration. Journal of Food Engineering 45(1):25-31.
104. Rastogi N.K., Niranjan K. 1998. Enhanced Mass Transfer During Osmotic Dehydration of High Pressure Treated Pineapple. Journal of Food Science 63(3):508-11.
105. Rastogi N.K., Raghavarao K.S., Balasubramaniam V.M., Niranjan K., Knorr D. 2007. Opportunities and Challenges in High Pressure Processing of Foods. Crit Rev Food Sci Nutr 47(1):69-112.
106. Rawson A., Patras A., Tiwari B.K., Noci F., Koutchma T., Brunton N. 2011. Effect of Thermal and Non Thermal Processing Technologies on the Bioactive Content of Exotic Fruits and Their Products: Review of Recent Advances. Food Research International 44(7):1875-87.
107. Reineke K., Mathys A., Knorr D. 2011. The Impact of High Pressure and Temperature on Bacterial Spores: Inactivation Mechanisms of Bacillus Subtilis above 500 Mpa. J Food Sci 76(3):M189-97.
108. Rendueles E., Omer M.K., Alvseike O., Alonso-Calleja C., Capita R., Prieto M. 2011. Microbiological Food Safety Assessment of High Hydrostatic Pressure Processing: A review. LWT - Food Science and Technology 44(5):1251-60.
109. Ritz M., Tholozan J.L., Federighi M., Pilet M.F. 2001. Morphological and Physiological Characterization of Listeria Monocytogenes Subjected to High Hydrostatic Pressure. Applied and environmental microbiology 67(5):2240-7.
110. Ross R. 2010. Wood Handbook: Wood as an Engineering Material. General technical report FPL; GTR-190. Madison, WI: U.S. Dept. of Agriculture, Forest Service, Forest Products Laboratory.
111. Sale A.J.H., Gould G.W., Hamilton W.A. 1970. Inactivation of Bacterial Spores by Hydrostatic Pressure. Journal of General Microbiology 60(3):323-34.
112. Seaman L. 1962. The Nature of Buckling in Thin Spherical Shells. Monograph Series: Watertown Arsenal Laboratories.
113. Sharma A. 2011. Microbial Adaptation to High Pressures-from Denial to a New Paradigm Shift. AGU Fall Meeting Abstracts 1:04.
114. Smelt J.P.P.M., Rijke A.G.F., Hayhurst A. 1994. Possible Mechanism of High Pressure Inactivation of Microorganisms. High Pressure Research 12(4-6):199-203.
115. Smith A.E., Moxham K.E., Middelberg A.P.J. 2000a. Wall Material Properties of Yeast Cells: Part Ii. Analysis. Chemical Engineering Science 55(11):2043-53.
116. Smith A.E., Zhang Z., Thomas C.R., Moxham K.E., Middelberg A.P.J. 2000b. The Mechanical Properties of Saccharomyces Cerevisiae. Proceedings of the National Academy of Sciences of the United States of America 97(18):9871-4.
117. Solecki R., Conant R.J. 2003. Advanced Mechanics of Materials. New York: Oxford University Press.

118. Stenson J.D., Hartley P., Wang C., Thomas C.R. 2011. Determining the Mechanical Properties of Yeast Cell Walls. Biotechnology Progress 27(2):505-12.
119. Stenson J.D., Thomas C.R., Hartley P. 2009. Modelling the Mechanical Properties of Yeast Cells. Chemical Engineering Science 64(8):1892-903.
120. Sun D.-W. 2005. Emerging Technologies for Food Processing. Amsterdam ; Boston: Elsevier Academic Press.
121. Syed Q.A., Buffa M., Guamis B., Saldo J. 2013. Lethality and Injuring the Effect of Compression and Decompression Rates of High Hydrostatic Pressure on Escherichia Coli O157:H7 in Different Matrices. High Pressure Research 33(1):64-72.
122. Tasi J. 1966. Effect of Heterogeneity on the Stability of Composite Cylindrical Shells under Axial Compression. AIAA Journal 4(6):1058-62.
123. Teo A.Y.L., Ravishankar S., Sizer C.E. 2001. Effect of Low-Temperature, High-Pressure Treatment on the Survival of Escherichia Coli O157:H7 and Salmonella in Unpasteurized Fruit Juices. Journal of Food Protection 64(8):1122-7.
124. Thakkar S.D. 2012. Effect of Processing on the Antioxidant Activity and Other Quality Parameters of Muscadine Grape Juice. [M.S.]: Rutgers University Available from: 1520048.
125. Thwaites J.J., Mendelson N.H. 1985. Biomechanics of Bacterial Walls: Studies of Bacterial Thread Made from Bacillus Subtilis. Proceedings of the National Academy of Sciences of the United States of America 82(7):2163-7.
126. Thwaites J.J., Surana U.C. 1991. Mechanical Properties of Bacillus Subtilis Cell Walls: Effects of Removing Residual Culture Medium. Journal of bacteriology 173(1):197-203.
127. Trejo Araya X.I., Hendrickx M., Verlinden B.E., Van Buggenhout S., Smale N.J., Stewart C., John Mawson A. 2007. Understanding Texture Changes of High Pressure Processed Fresh Carrots: A Microstructural and Biochemical Approach. Journal of Food Engineering 80(3):873-84.
128. Van den Broeck I., Ludikhuyze L.R., Van Loey A.M., Hendrickx M.E. 2000. Inactivation of Orange Pectinesterase by Combined High-Pressure and -Temperature Treatments: A Kinetic Study. Journal of Agricultural and Food Chemistry 48(5):1960-70.
129. Van Opstal I., Vanmuysen S.C., Wuytack E.Y., Masschalck B., Michiels C.W. 2005. Inactivation of Escherichia Coli by High Hydrostatic Pressure at Different Temperatures in Buffer and Carrot Juice. Int J Food Microbiol 98(2):13-.
130. Whitney B.M. 2005. Efficacy of High Pressure Processing in Combination with Chemical Preservatives for the Reduction of Escherichia Coli O157:H7 and Salmonella in Apple Juice and Orange Juice. [M.S.]. Blacksburg, Virginia: Virginia Polytechnic Institute and State University.
131. Wong P.T.T., Heremans K. 1988. Pressure Effects on Protein Secondary Structure and Hydrogen Deuterium Exchange in Chymotrypsinogen: A Fourier Transform Infrared Spectroscopic Study. Biochimica et Biophysica Acta (BBA) - Protein Structure and Molecular Enzymology 956(1):1-9.

132. Wu P.G., Brand L. 1994. Resonance Energy Transfer: Methods and Applications. Analytical Biochemistry 218(1):1-13.
133. Yen G.-C., Lin H.-T. 1996. Comparison of High Pressure Treatment and Thermal Pasteurization Effects on the Quality and Shelf Life of Guava Puree. International Journal of Food Science & Technology 31(2):205-13.
134. Zhang L. 2011. Effect of Package Dimensions and Food Product Properties on Non-Uniformity of Microbial Inactivation During High-Pressure High-Temperature (Hpht) Process a Numerical Study. Rutgers University. Graduate School--New Brunswick.,. p. xvi, 102 p.
135. Zook C.D., Parish M.E., Braddock R.J., Balaban M.O. 1999. High Pressure Inactivation Kinetics of Saccharomyces Cerevisiae Ascospores in Orange and Apple Juices. Journal of Food Science 64(3):533-5.